

DTIC FILE COPY

0

AD-A196 871

REPORT DOCUMENTATION PAGE		READ INSTRUCTIONS BEFORE COMPLETING FORM
1. REPORT NUMBER AFIT/CI/NR 88- 83	2. GOVT ACCESSION NO.	3. RECIPIENT'S CATALOG NUMBER
TITLE (and Subtitle) MATHEMATICAL MODEL OF A TIMBER BRIDGE GUARD RAIL SYSTEM		5. TYPE OF REPORT & PERIOD COVERED MS THESIS
AUTHOR(s) MARK S. MALONE		6. PERFORMING ORG. REPORT NUMBER
PERFORMING ORGANIZATION NAME AND ADDRESS AFIT STUDENT AT: COLORADO STATE UNIVERSITY		8. CONTRACT OR GRANT NUMBER(s)
CONTROLLING OFFICE NAME AND ADDRESS		10. PROGRAM ELEMENT, PROJECT, TASK AREA & WORK UNIT NUMBERS
14. MONITORING AGENCY NAME & ADDRESS (if different from Controlling Office) AFIT/NR Wright-Patterson AFB OH 45433-6583		12. REPORT DATE 1988
		13. NUMBER OF PAGES 94
		15. SECURITY CLASS. (of this report) UNCLASSIFIED
		15a. DECLASSIFICATION/DOWNGRADING SCHEDULE
16. DISTRIBUTION STATEMENT (of this Report) DISTRIBUTED UNLIMITED: APPROVED FOR PUBLIC RELEASE		
17. DISTRIBUTION STATEMENT (of the abstract entered in Block 20, if different from Report) SAME AS REPORT		
18. SUPPLEMENTARY NOTES Approved for Public Release: IAW AFR 190-1 LYNN E. WOLAVER Dean for Research and Professional Development Air Force Institute of Technology Wright-Patterson AFB OH 45433-6583		
19. KEY WORDS (Continue on reverse side if necessary and identify by block number)		
20. ABSTRACT (Continue on reverse side if necessary and identify by block number) ATTACHED		

DTIC
EXTRACTED
AUG 04 1988
H

ABSTRACT OF THESIS

MATHEMATICAL MODEL OF A TIMBER BRIDGE GUARDRAIL SYSTEM

△ A timber bridge guardrail system, subjected to static loads, was twice mathematically modeled as a beam on elastic supports. The initial model possessed uncoupled discrete spring supports representing the support provided to the guardrail by the posts. The second model contained coupled spring supports, the coupling being provided by the bridge deck structure to which the line of guardrail posts are attached. The stiffnesses of the spring supports for both models were determined experimentally by transversely loading each post of a timber guardrail section of a longitudinal laminated deck bridge after the guardrail member was removed. Using these stiffnesses, each model was utilized to predict the deflections of the complete test specimen (with the guardrail reattached). The first model was inaccurate, producing unacceptably large predictions of the actual deflections. The second model considerably improved the prediction of the deflected shape and magnitude of the deflections. For the representative load condition (rail loaded at center post location) the latter model

yielded displacements within 13% of the measured values as compared to 34% for the former model. *See model. This*

... RAIL ... program

Mark S. Malone
Department of Civil Engineering
Colorado State University
Fort Collins, CO 80523
Spring 1988



Accession For	
NTIS CR&I	<input checked="" type="checkbox"/>
DTIC TAB	<input type="checkbox"/>
Unannounced	<input type="checkbox"/>
Justification	
By _____	
Distribution/	
Availability Codes	
Dist.	Avail and/or Special
A-1	

THESIS

MATHEMATICAL MODEL OF A TIMBER
BRIDGE GUARDRAIL SYSTEM

Submitted by

Mark S. Malone

Department of Civil Engineering

In partial fulfillment of the requirements

for the Degree of Master of Science

Colorado State University

Fort Collins, Colorado

Spring 1988

COLORADO STATE UNIVERSITY

DECEMBER 14 19 87

WE HEREBY RECOMMEND THAT THE THESIS PREPARED UNDER OUR
SUPERVISION BY MARK SIDNEY MALONE

ENTITLED MATHEMATICAL MODEL OF A TIMBER BRIDGE GUARDRAIL SYSTEM

BE ACCEPTED AS FULFILLING IN PART REQUIREMENTS FOR THE
DEGREE OF MASTER OF SCIENCE

Committee on Graduate Work

Patricia J. DeBeane

Martin E. Cissell

Richard M. Gutkowski
Adviser

Shane Oehl
Department Head

ABSTRACT OF THESIS

MATHEMATICAL MODEL OF A TIMBER BRIDGE GUARDRAIL SYSTEM

A timber bridge guardrail system, subjected to static loads, was twice mathematically modeled as a beam on elastic supports. The initial model possessed uncoupled discrete spring supports representing the support provided to the guardrail by the posts. The second model contained coupled spring supports, the coupling being provided by the bridge deck structure to which the line of guardrail posts are attached. The stiffnesses of the spring supports for both models were determined experimentally by transversely loading each post of a timber guardrail section of a longitudinal laminated deck bridge after the guardrail member was removed. Using these stiffnesses, each model was utilized to predict the deflections of the complete test specimen (with the guardrail reattached). The first model was inaccurate, producing unacceptably large predictions of the actual deflections. The second model considerably improved the prediction of the deflected shape and magnitude of the deflections. For the representative load condition (rail loaded at center post location) the latter model

yielded displacements within 13% of the measured values as compared to 34% for the former model.

Mark S. Malone
Department of Civil Engineering
Colorado State University
Fort Collins, CO 80523
Spring 1988

ACKNOWLEDGMENTS

I wish to express my appreciation to my advisor, Dr. Richard M. Gutkowski, and to the members of my graduate committee, Dr. Marvin E. Criswell and Dr. Patrick J. Pellicane for their insight, guidance, suggestions, and assistance during the preparation of this thesis. I also thank my co-researcher Jean Francois Kalin, with whom I worked closely in the Structural Engineering Laboratory at the Engineering Research Center.

Wheeler Consolidated, Inc., of Des Moines, Iowa, provided the timber guardrail test specimen for the project, and for this important item I am most appreciative.

Also, I am obliged to the United States Air Force Institute of Technology for fully sponsoring me during my Master's degree program at Colorado State University.

Finally, I am eternally grateful to my wife, Rochelle, who not only provided patient typing support, but also convinced me to strive for an advanced degree in the first place.

TABLE OF CONTENTS

<u>Chapter</u>		<u>Page</u>
	ABSTRACT	iii
	ACKNOWLEDGMENTS.	v
	LIST OF TABLES	viii
	LIST OF FIGURES.	ix
1	INTRODUCTION	1
	1.1 Background.	1
	1.1.1 Timber Bridges and Guardrails. . .	2
	1.1.2 Research Project to Develop Mathematical Model	3
	1.2 Other Guardrail Tests and Models.	4
	1.2.1 Full Scale Crash Tests	4
	1.2.2 Static Load Tests and AASHTO Requirements	6
	1.3 Timber Bridge Test Specimen	8
	1.4 Beam on Elastic Supports Model.	9
	1.4.1 Description of Modeling.	9
	1.4.2 Inappropriateness of Beam on Elastic Foundation Model	13
2	SIMPLE LATERAL SPRINGS MODEL - DIAGONAL STIFFNESS MATRIX	17
	2.1 Model Description	17
	2.2 Spring Constants for Model.	18
	2.2.1 Test Setup and Procedure	18
	2.2.2 Results.	22
	2.3 Matrix Structural Analysis Predictions (GTSTRUDL).	28
	2.3.1 Model Geometry and Loads	28
	2.3.2 GTSTRUDL Model Deflections	30
	2.4 Model Validation.	30
	2.4.1 Test Setup and Procedure	31
	2.4.2 Comparison of Results and Conclusions.	33
3	SIMPLE LATERAL SPRINGS MODEL - FULL STIFFNESS MATRIX	40
	3.1 Model Description	40
	3.2 Stiffness Matrix for Model.	41
	3.2.1 Test Setup and Procedure	42
	3.2.2 Reduction of Data.	44
	3.2.3 Results.	46

<u>Chapter</u>	<u>Page</u>	
3.3	Matrix Structural Analysis	
	Predictions (Program RAIL)	47
3.3.1	Introduction	47
3.3.2	Flexibility Matrix Inversion	48
3.3.3	Model Geometry and Loads	48
3.4	Model Validation.	50
3.4.1	Rail Test Setup and Procedure.	50
3.4.2	Comparison of Results and Conclusions.	51
3.5	Comparison of Laboratory Rail Tests	64
3.6	Load Sharing Among Rail Posts	67
4	SUMMARY AND CONCLUSIONS.	69
4.1	Summary	69
4.2	Conclusions	71
4.3	Recommendations	72
	REFERENCES	75
	APPENDIX A - Effective Beam Length and Post Spacing Calculations.	78
	APPENDIX B - GTSTRU DL Input File	80
	APPENDIX C - BASIC Data Reduction Routine.	84
	Program RAILDATA Listing.	85
	Sample Input Data File.	86
	Sample Output Product	87
	APPENDIX D - Program RAIL.	88
	Sample Input Data File.	89
	Sample Output Product	90

LIST OF TABLES

<u>Table</u>		<u>Page</u>
2.1	Summary of Spring Constants for Rail Posts. . . .	26
2.2	Summary of GTSTRUDL Deflection Predictions. . . .	31
2.3	Summary of Laboratory Rail Test Results	34
2.4	Comparison of Rail Test Results with GTSTRUDL Predictions	35
3.1	Full Flexibility Matrix for Post System	45
3.2	Adjusted Flexibility Matrix for Post System . . .	46
3.3	Full Stiffness Matrix for Post System	48
3.4	Summary of Program RAIL Deflection Predictions. .	50
3.5	Summary of Laboratory Rail Test Results for Load at End Post (Post 1)	52
3.6	Summary of Laboratory Rail Test Results for Load at Quarter Post (Post 2)	53
3.7	Summary of Laboratory Rail Test Results for Load at Center Post (Post 3).	54
3.8	Comparison of Rail Test Results with Program RAIL Predictions.	58

LIST OF FIGURES

<u>Figure</u>	<u>Page</u>
1.1 Treated Timber Bridge Rail Test Specimen.	10
1.2 Typical Timber Guardrail-to-Deck Connections.	11
1.3 Beam on Elastic Supports Model.	12
2.1 Test Specimen Orientation within Structural Engineering Laboratory.	19
2.2 Transverse Loading of Rail Posts.	20
2.3 Deflection Measurements Using DCDT's.	21
2.4 Load-Deflection Hysterisis Effect	23
2.5 Calculating Spring Constants for Posts.	24
2.6 Components of Center Post Deflection.	26
2.7 End Post Deflection	27
2.8 Schematic of GTSTRUDL Timber Rail Model	29
2.9 Rail Test Load Application.	32
2.10 Comparison of Rail Test Results with GTSTRUDL Predictions for Load at Post 1.	36
2.11 Comparison of Rail Test Results with GTSTRUDL Predictions for Load at Post 2.	37
2.12 Comparison of Rail Test Results with GTSTRUDL Predictions for Load at Post 3.	38
3.1 Rail on Interacting Springs Model	42
3.2 Determination of Full Flexibility Matrix for Post System	43
3.3 Schematic of Program RAIL Timber Rail Model	49

<u>Figure</u>		<u>Page</u>
3.4	Effect of Load Position on Deflected Shape of Test Specimen Rail During Laboratory Rail Test. .	55
3.5	Effect of Load Magnitude on Deflected Shape of Test Specimen Rail During Laboratory Rail Test. .	56
3.6	Comparison of Rail Test Results with Program RAIL Predictions for Load at Post 1	59
3.7	Comparison of Rail Test Results with Program RAIL Predictions for Load at Post 2	60
3.8	Comparison of Rail Test Results with Program RAIL Predictions for Load at Post 3	61
3.9	Increase in Moment Arm of Lateral Load About Base of Post.	62
3.10	Relative Torsional Stiffness of Outer Deck Members.	63

Chapter 1

INTRODUCTION

1.1 Background

Over the past several decades the condition of the infrastructure of the United States has deteriorated nearly to the point of collapse, according to Pat Choate, a congressional adviser and senior policy analyst for TRW, Inc. (18). This country's streets, highways, bridges, sewers, water mains, utilities, dams, buses and subways have all felt the adverse effects of numerous local, state, and federal fiscal crises as well as outright neglect. As a result, it is estimated that 2.75 trillion dollars would have to be spent this decade on repairing the infrastructure just to maintain the current level of service on public facilities (18).

Of this amount, approximately 35% is needed to repair the nation's rural highways and bridges. Because of an intense emphasis on the Interstate System, only very limited funds have been available for rural bridges during its construction. As a result of the low rate of replacement of such bridges in rural systems largely built in the 1920's and 1930's, over 90 percent of all rural bridges now in

service were built before 1935, and therefore have exceeded their design service life (14).

Fortunately, governmental efforts are now underway to improve the condition of bridges of all types and materials, including timber bridges. The Federal Highway Administration has established and been maintaining a National Bridge Inventory to provide a common reference for determining repair and replacement requirements. The Federal Highway Bridge Replacement and Rehabilitation Program allows states to compete for bridge maintenance funding. Legislation also stipulates that a minimum of 15 percent and a maximum of 35 percent of federally apportioned funds be spent for bridges off the Federal-aid system (5,9).

1.1.1 Timber Bridges and Guardrails

The highway system in the U.S. contains a large number of existing timber bridges. Over 71,000 highway bridges use timber as the main component. Another 8,500 timber bridges are in place within the National Forest System (5,9).

Many features of wood give it a distinct advantage as a construction material for short span bridges. Wood is lightweight, with considerable reserve strength under dynamic loads. Sections of timber bridges can be prefabricated, then placed into position at the construction site. Also, timber members can be pressure-treated with preservatives to provide decay resistance (15,8). Finally, the cost of timber bridges is competitive with the cost of bridges made of other materials (25,20).

An important technical shortcoming of timber bridges is the unavailability of timber guardrails that have demonstrated successful performance, as defined by the American Association of State Highway and Transportation Officials (AASHTO) (21) requirements, in standard vehicle crash tests (5,9). Consequently, the unavailability of a timber guardrail system meeting AASHTO design criteria is a major obstacle to the use of timber bridges for new construction as well as for replacement projects. Bridge projects dependent upon matching federal funds must satisfy AASHTO requirements to obtain the federal funds. This effectively eliminates timber as a construction material for bridges in which the guardrail is an essential structural component (5,9).

An analytical model which would accurately predict the performance of a timber bridge rail in a full-scale crash test, could help encourage a company or government agency to invest in such a test. Conduct of such tests without some confidence of success or ability to generalize the results is a costly option as a test without backup analytical tools would provide information only on the guardrail configuration tested. Thus the need for a rational mathematical model for timber bridge guardrail systems subjected to impact loads is a pressing one.

1.1.2 Research Project to Develop Mathematical Model

The research documented in this report was conducted as part of a larger project supported by the USDA Competitive

Grant program. The goal of that research project and subsequent studies is to provide a means for predicting the behavior of timber guardrails under static load and to initiate studies of impact loading. To fully accomplish the latter goal, the long term research has been divided into three phases. In each phase, increasing refinement will be made by progressive development of three models termed: 1) Static Load Model, 2) Semi-Empirical Impact Load Model, and 3) Rigorous Impact Load Model. The objective of Phase 1 is to successfully model a timber bridge guardrail as a continuous member with elastic supports. Phase 2 will extend the Static Load Model to include impact loading and resistance capacity. If necessary, Phase 3 will model the structural configuration of the rail post assembly in great detail.

This report describes the development of an initial mathematical model of a timber guardrail system subjected to static loads and is a part of Phase 1 of the overall research effort described above. Before creating the static load model, a search of the literature was conducted to determine if any timber guardrails had been mathematically modeled or load tested.

1.2 Other Guardrail Tests and Models

1.2.1 Full Scale Crash Tests

A literature search revealed no full-scale crash tests of timber guardrails or bridge rails. However, many types of steel and concrete guardrails and bridge rails have been

crash tested. Bronstad, et al., have reported the results of full scale crash tests on 11 different barrier systems for an 1800 pound test vehicle (4). The 11 longitudinal barrier systems included 5 guardrail systems, 2 median barriers and 4 bridge railings. The types of barriers included wire rope cables, steel "W beams", steel "thrie beams" (similar to "W beams" but wider), steel box beams, and concrete parapets. The findings indicate all systems met impact test requirements for an 1800 pound car traveling at 60 mph and striking the system at a 15-degree angle.

Hirsch and Fairbanks have reported the full scale testing of a modified Texas Type T5 concrete traffic rail to redirect an 80,000-pound tractor and tank trailer (13). A continuous concrete beam was mounted on concrete posts on the top of the concrete parapet. This tall bridge rail was able to contain and smoothly redirect the test vehicle at 50 mph and a 15-degree angle of impact.

Bronstad and McDevitt have designed and crash tested flexible, damage-resistant, self-restoring barriers (SERB) for vehicles ranging in weight from 1800 to 40,000 pounds (3). The SERB median barrier is constructed of two steel thrie beam elements bolted to two truss web members and hung on specially designed posts spaced at 12-ft 6-inch centers. The design permits a 3-1/2 inch lateral translation and a 6 inch vertical translation before bottoming. The barrier is designed to return to its pre-impact position after the collision. The SERB median barrier successfully contained

and smoothly redirected the 40,000-lb intercity bus and kept the bus upright during a 57 mph impact at an angle of 14 degrees to the rail. The SERB system contained and redirected the 1800-lb car with essentially no damage to the rail.

Denman and Krage have designed and crash tested a transitioning end treatment (TREND) system to protect errant motorists from the hard point presented at the end of rigid or semi-rigid barriers (7).

1.2.2 Static Load Tests and AASHTO Requirements

In addition to the many impact tests of bridge rails reported in the literature, static load test results for concrete and timber bridge rail systems were also reported.

AASHTO specifies design static loads on bridge railings according to estimates of forces imposed on railings by traffic under normal operations and on railings during collisions by automobiles (1).

AASHTO requires that a traffic rail system resist an outward transverse design load, P , of 10 kips applied at a post location at the guardrail height. This design load shall be increased by the factor C ,

$$C = 1 + (h - 33) / 18 \geq 1 \quad (1.1)$$

when the height, h , of the rail exceeds 33 inches (2'-9"). While resisting the outward 10 kip transverse load, the rail system must simultaneously withstand a longitudinal load of one-half the transverse load. The longitudinal load shall be divided among not more than four posts in a continuous

rail length. Finally, the rail system must also be able to carry an inward transverse load at a post of one-fourth the outward transverse load. The AASHTO requirements for traffic railings conclude by stating that any railing configurations which have been successfully tested by full scale impact tests are exempt from these static load requirements (21).

Arnold has presented the results of static load tests of concrete bridge rails attached to concrete bridge decks (1). The central interest of the study was deck failure patterns when the rail posts were loaded. Peak static loads ranging from 18.6 kips to 45 kips were applied to Texas Bridge Railing Types T101, T202, and T5. Recommendations to reduce the damage to concrete decks included: 1) increase steel reinforcement in decks near the edges and posts, 2) increase thickness of decks, and 3) increase post-to-edge-of-deck distance.

In November 1976, Weyerhaeuser Company conducted static load tests of three of their bridge rail systems -- a "traffic rail", a "traffic barrier", and a "safety rail". The traffic rail consisted of a 21" deep glulam wheel rail and a 6 3/4" deep glulam top rail attached to 6 3/4" x 7 1/4" solid-sawn timber rail posts. The traffic barrier was shaped like the standard New Jersey concrete parapet, but consisted of glulams bolted to the deck. The safety rail was similar in shape to the traffic rail but had a smaller wheel rail, top rail, and rail posts.

The first two rails were designed and loaded according to the 1975 Interim Specifications of the 1973 AASHTO standard. The safety rail was not based on either of these code documents. Weyerhaeuser concluded that the traffic rail and traffic barrier successfully passed the 1975 AASHTO requirements for static loads and that bolted, treated-timber construction was good for bridge rails because of timber strength, flexibility, and load sharing (11). No mathematical modeling was formulated to predict the test outcome.

No analysis models specific to timber guardrail systems were found in the literature. Mathematical modeling of guardrail systems using other materials was also searched for in the literature using the Engineering Index of Abstracts. Paul N. Roscke, from the University of Texas at El Paso, in a 1986 paper entitled "Crash Performance Prediction of a Vehicle Against an Energy-Absorbing Bridge Guardrail" described his efforts at improving the capabilities of a bridge rail computer program called CRUNCH (19). However, CRUNCH is a complex finite-element model for dynamic loadings. A simple, bridge rail computer model for static loadings was not found.

1.3 Timber Bridge Test Specimen

In order to validate any mathematical model of a timber bridge rail, an actual bridge rail specimen for testing was needed. A 26-ft long section of a longitudinal laminated

deck bridge, complete with curb and rail system attached was used (see Figure 1.1) .

The deck section consists of 16 solid sawn 4" x 12" boards spiked together. The curb block is two solid sawn 6" x 12" members bolted together. The five rail posts are solid sawn 8" x 12" sections bolted and spiked to the curb-block and deck, respectively. The rail is a 6" x 10 5/8" glulam beam with 4 laminates.

The wood in the test specimen is creosote-treated Douglas-Fir Larch. The deck members fall into the National Design Specifications (NDS) (16) category Grade #1 Structural Joists and Planks, 2" to 4" Thick, 5" and Greater in Width. The rail posts are in the NDS category Beams and Stringers with a grade of Dense Select Structural. The glulam rail falls under the NDS category 24F-V4 for Douglas Fir and Western Larch (22).

Because the rail/deck system was delivered as an assemblage, it could not easily be disassembled and reassembled, especially for components connected with drive spikes. Thus no tests for the properties of individual members were conducted.

1.4 Beam on Elastic Supports Model

1.4.1 Description of Modeling

Any mathematical model of a timber guardrail system obviously should be accurate. In addition to accuracy, a model should also demonstrate simplicity whenever possible, for ease of use and understanding.

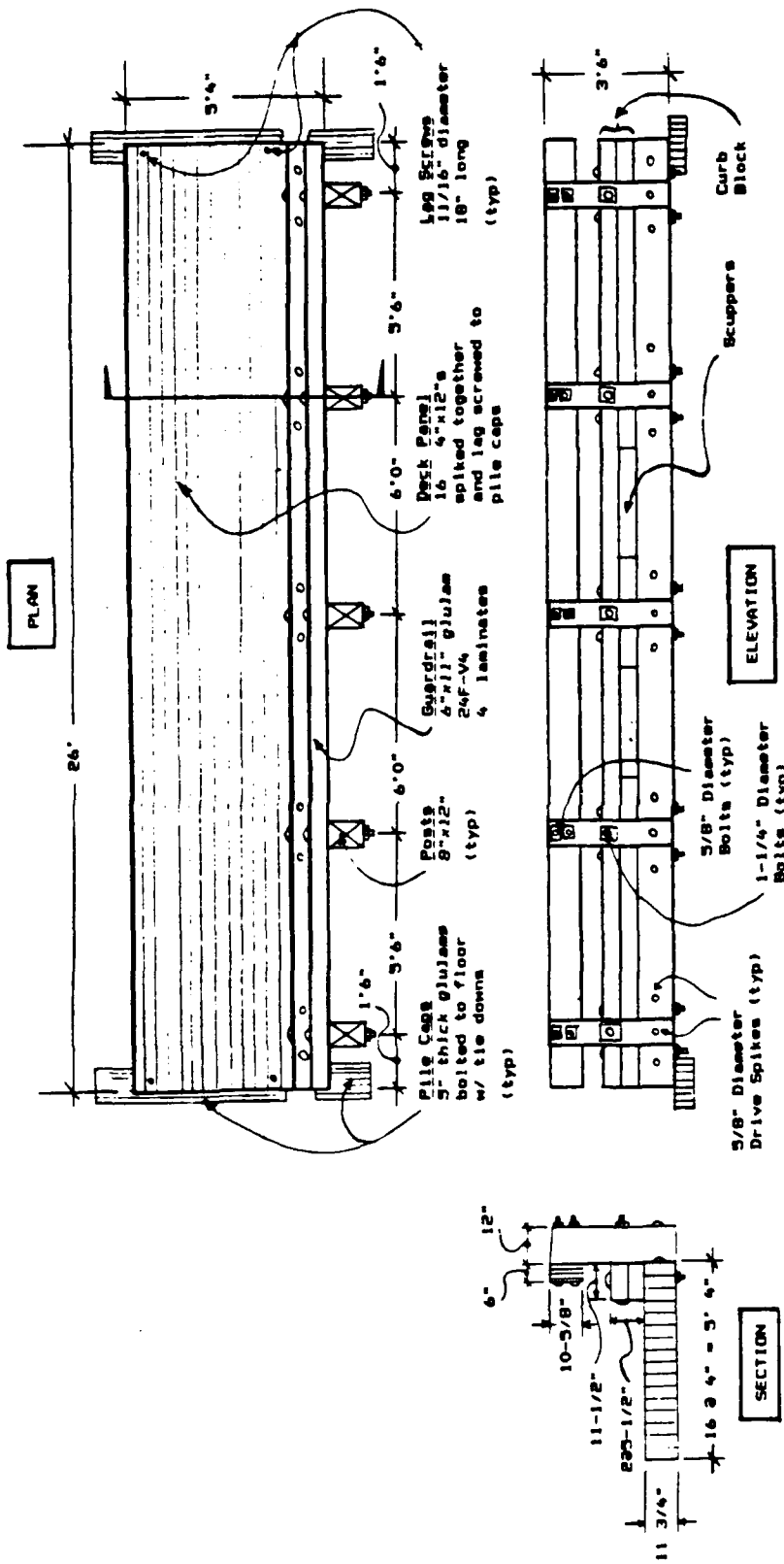


Figure 1.1 Treated Timber Bridge Rail Specimen

Unfortunately, timber is a construction material exhibiting a high degree of variability in its physical and mechanical properties. In addition, the connection details of a guardrail system to a timber bridge decking are quite complex, requiring bolts, spikes, and blocks (see Figure 1.2) .

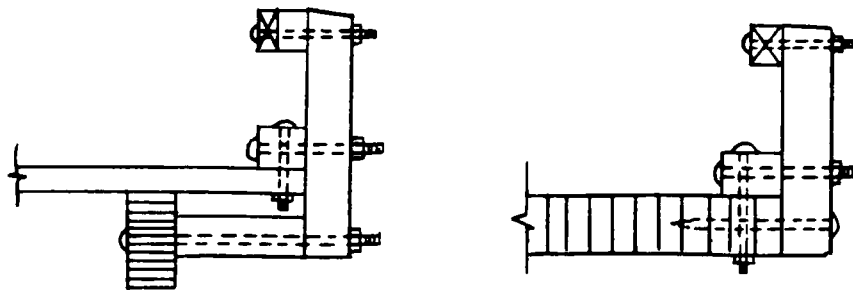


Figure 1.2 Typical Timber Guardrail-to-Deck Connections

A rigorous structural representation of a guardrail system would be to mathematically model it as a framework representing all components and connections present. However, mechanical fasteners are subject to relative motion between the connected parts. Local crushing of wood around the connection is possible, and loosening of connectors may even occur under repeated loading (5,9). For these and other reasons, even a rigorous model of a timber guardrail system would likely necessitate extensive studies of the behavior of each individual component and connection detail.

Further, the connection details and member sizes generally differ for the various timber guardrail systems currently available.

Due to the present unavailability of test data needed in a rigorous model, it was decided to initially model the guardrail system as a beam (the rail) on an elastic supports consisting of uncoupled discrete springs supports (the posts), see Figure 1.3 . A particular guardrail system presently being used in some timber bridge construction was tested to verify the model. However, as developed, the mathematical modeling technique is not specific to any

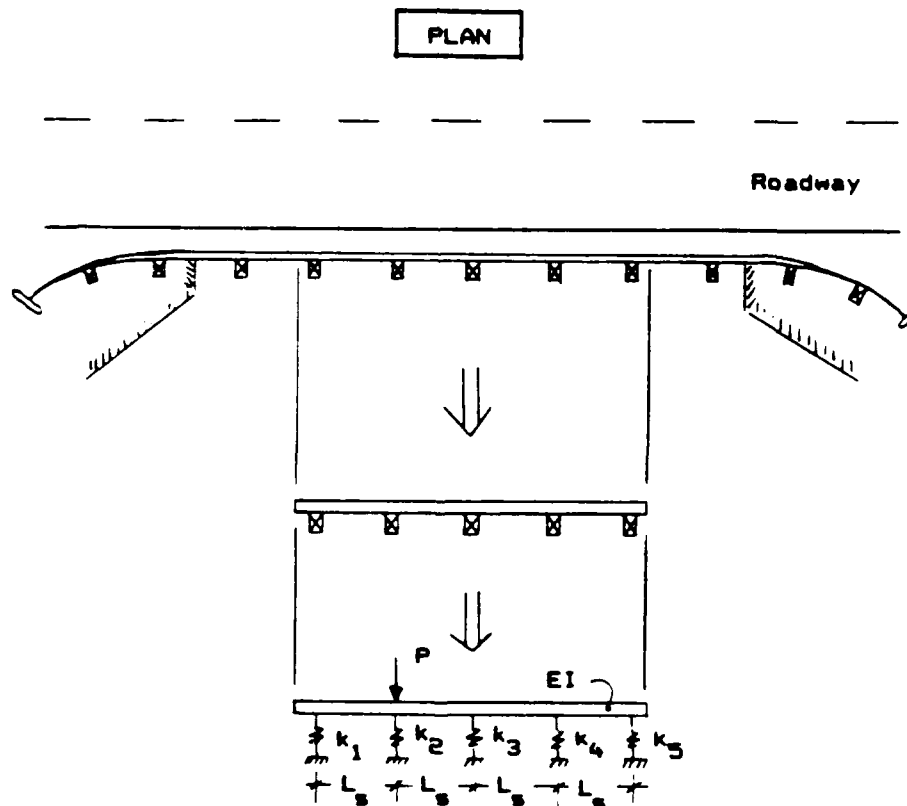


Figure 1.3 Beam on Elastic Supports Model

given guardrail system configuration. The process of creating and experimentally verifying this model is the subject of Chapter 2.

During the initial model validation, it was observed that the configuration of rail posts attached directly to a longitudinal-laminated deck causes the posts to behave as springs which significantly interact with each other, mainly through the torsional action of the curb block and deck, instead of as springs which are effectively independent of each other. The initial model was later modified to include this interaction among springs. The modified model is presented and discussed in Chapter 3.

1.4.2. Inappropriateness of Beam On Elastic Foundation Model

Before it was decided to model the guardrail as a beam on discrete spring supports, it was thought that the test specimen might be modeled as a beam on elastic foundation, in which the discrete supports are represented as a continuous support (i.e. foundation). Therefore, the appropriateness of a beam on elastic foundation model was investigated.

In the literature, the subject of beams on elastic foundation is covered in detail by M. Hetenyi in his 1946 book (11). According to Hetenyi, for beams on closely spaced elastic supports (e.g. railroad rail on crossties) the discrete supports can be approximated by a continuous distributed foundation with a modulus of:

Units

$$k = K/L_s \quad (F/L^2) \quad (\text{Force per unit deflection per unit length of beam})$$

where K = stiffness of the springs, (Force/unit deflection)

L_s = spacing of the springs, (Length)

(Hetenyi actually attributed this approximation to Timoshenko in 1915). Hetenyi also classified beams of finite length into three groups:

- I. Short Beams, with $\beta L < \pi/4$
- II. Medium Beams, with $\pi/4 < \beta L < \pi$
- III. Long Beams, with $\pi < \beta L$

where $\beta = (k/4EI)^{1/4}$, (1/L); this relative stiffness parameter is sometimes denoted as λ

L = beam length, (L)

k = spring coefficient, K/L_s , (F/L²)

More recently, Boresi and Sidebottom (2,5) have divided finite length beams on elastic foundations into two groups:

- I. "Short" Beams, with $L < 3\pi / 2\beta$
- II. "Long" Beams, with $L \geq 3\pi / 2\beta$

where $\beta = (k/4EI)^{1/4}$, (1/L)

L = beam length, (L)

k = spring coefficient, K/L_s , (F/L²)

These authors state that the infinite length beam on elastic foundation theory provides a reasonable approximate solution for a "Long" ($L \geq 3\pi / 2\beta$) finite length beam.

Boresi and Sidebottom also state that for a foundation of equally spaced discrete springs, the equivalent distributed spring constant, $k = K/L_s$, is a sufficiently good approximation (about 5% error on maximum deflections) as long as L_s , the space between springs, does not exceed $\pi / 4\beta$.

To examine the applicability of the beam on elastic foundation theory to the timber bridge rail specimen, the effective length of the rail and the spring (post) spacings were checked. Certain assumptions had to be made to compute these parameters. The springs (posts) were all assumed to have the same spring constant and the spring spacing was assumed to be constant. Average values for spring constants and spring spacings were used in the computations, see Appendix A.

Results of the calculations showed that the rail had an effective length, L'' , of 345 inches. The $L'' = 345$ in. was slightly greater than the dividing parameter between "short" and "long" beams, $3\pi / 2\beta = 343$ in. This placed the rail barely into the "long" beam category according to Boresi and Sidebottom criteria. This effective length of beam was very close to a length where beam on elastic foundation theory begins to be an "unreasonable" approximation. Also, the average spring (post) spacing of 69 inches was 21% larger than "reasonable", and some error, probably significant, would have been introduced by applying beam on elastic foundation theory to the particular test

specimen. Therefore it was decided to, instead, model the timber guardrail as a beam on essentially equally spaced discrete elastic springs.

Chapter 2

SIMPLE LATERAL SPRINGS MODEL - DIAGONAL STIFFNESS MATRIX

This chapter describes the process of creating, testing and validating a model of a bridge guardrail as a beam on a set of independent linearly elastic lateral springs.

2.1 Model Description

The modeling of the guardrail posts as independent springs was thought to be the simplest practical representation possible for the behavior of a timber bridge rail. The ability of this simple model to adequately model the system was initially unknown and was to be determined. The model consists of a beam (the glulam rail itself) resting on five linear, uncoupled springs (the posts), see Figure 1.3 . Since the springs are assumed to act independently and provide lateral resistance only, the stiffness matrix of the post system (minus the rail) has entries only on the main diagonal.

Each post was represented as a linear, lateral (perpendicular to the rail) spring with a measured spring constant, k , having units F/L (e.g. pounds of load per inch of deflection). In this initial model, the torsional rigidity of each post was ignored, as was the longitudinal (parallel to the rail) stiffness of each post. The next

step was to experimentally determine what spring constant to assign each post.

2.2 Spring Constants for Model

2.2.1 Test Setup and Procedure

The spring constant for each post was obtained by testing the existing timber bridge rail specimen. The bridge specimen was delivered to Colorado State University's Engineering Research Center (ERC) as a single unit, including deck, curb block, posts and rail. The specimen was placed at the north end of the Structural Engineering Laboratory, on two simulated pile caps (see Figure 2.1).

Each pile cap was bolted to the laboratory floor using 2-inch diameter bolts screwed into two tie-down locations in the floor. The pattern of these tie-down locations in the floor of the laboratory necessitated the placement of the bridge at the north end. The bridge deck was connected to each pile cap with 2 lag screws 18 inches long, to prevent the bridge from displacing during testing.

After the railing member member was removed, a ten thousand pound (10 kip) capacity electrically driven winch was used to apply transverse loads to one of the south three rail posts via a wire rope cable (See Figure 2.2) . This winch can be moved along a steel railing parallel with the bridge, but because of the position of the bridge in the northern part of the laboratory, only the center post, a quarter post and an end post could be loaded (see Figure 2.1) .

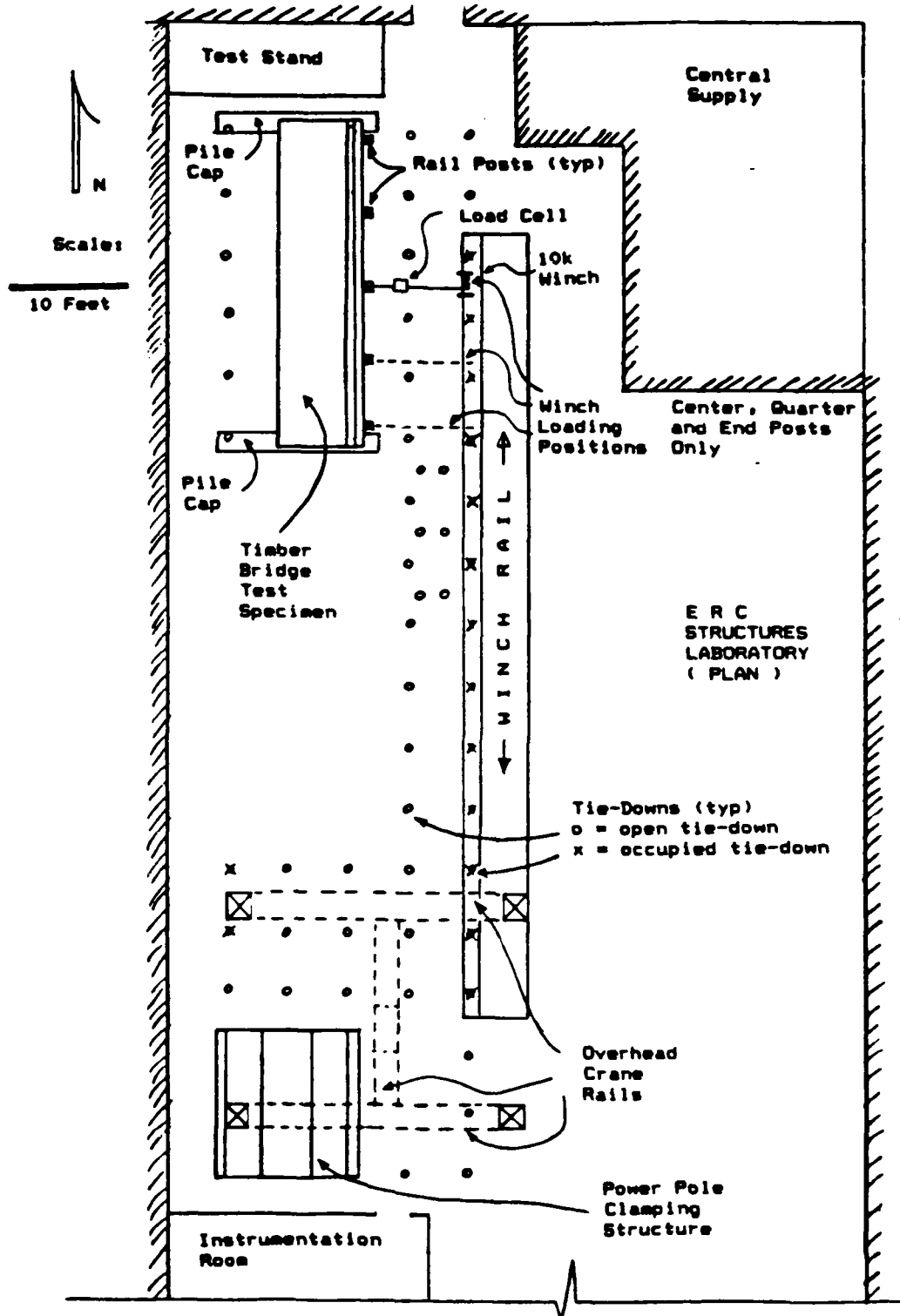


Figure 2.1 Test Specimen Orientation within Structural Engineering Laboratory

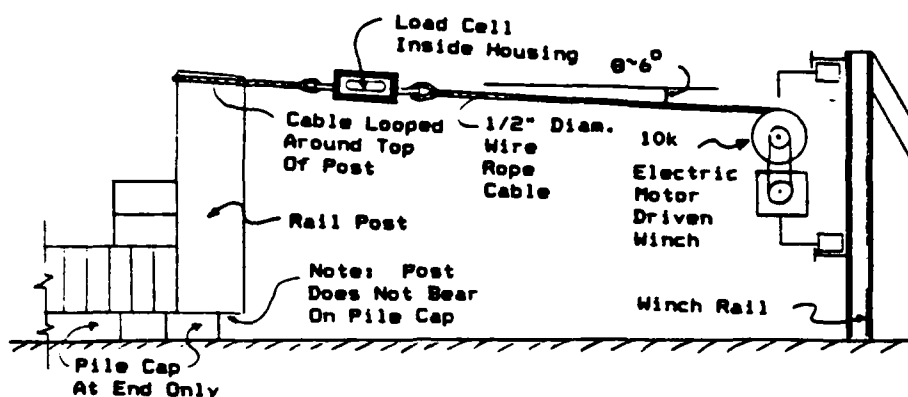


Figure 2.2 Transverse Loading of Rail Posts

Plans are to add more tie-downs to the Structural Engineering Laboratory and to move the bridge to a more desirable location. For the purposes of the initial model, a plane of structural symmetry through the center post and perpendicular to the rail was assumed. This assumption resulted in the spring constant values of the end and quarter posts on the south part of the bridge being also used as the spring constant values of the end and quarter posts on the north part of the bridge. The validity of this assumption is discussed further in Section 3.2.1.

For determining spring constants each post was separately loaded. The wire rope winch cable was aligned with the post and looped over the top of the post. The winch applied a slowly increasing load, and the deflection at the top of the loaded post was measured. The applied load was measured with an electronic load cell in the wire rope cable

system (see Figure 2.2.). The deflections were measured with Direct Current Displacement Transducers (DCDT's), as shown in Figure 2.3 .

The DCDT's produce changes in voltage proportional to displacement. These voltage changes as measured by data acquisition instrumentation were later converted to displacements using the calibration factor for each DCDT.

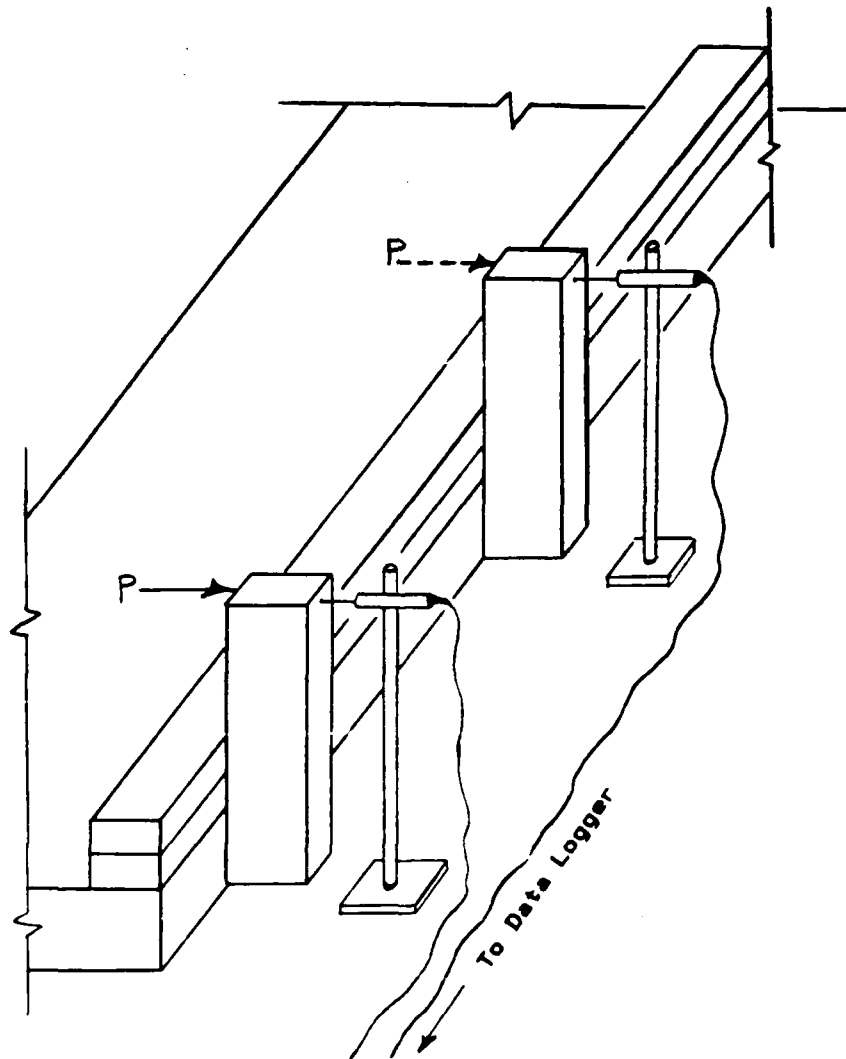


Figure 2.3 Deflection Measurements Using DCDT's

The instrumentation room of the Structural Engineering Laboratory housed the amplifier which provided the voltage excitation to the DCDT's and to the load cell, along with the signal processing and recording equipment. The load-deflection curve was plotted for the loaded post using a pen plotter which received input from the load cell and from a DCDT. An electronic data logger took instantaneous readings of the load cell and DCDT voltages at about five second intervals and recorded these readings on paper tape.

It was decided that a 0 to 3 kip load range would be used for determining spring constants. Non-destructive evaluation of the bridge rail system was planned to enable later utilization of the system for static loads both parallel to and at an angle to the rail. The 3 kips test load was felt to be far enough below the design load of 10 kips to prevent either damage or permanent deformation. After completion of the various planned tests at the 3 kip load level, proof testing up to AASHTO load levels is planned.

2.2.2 Results

Each of the three accessible posts was loaded and unloaded eight times. The load-deflection plot shows a hysteresis effect in which the first loading and unloading curve formed a loop which crept upward on the graph for the first two or three cycles (see Figure 2.4). It is believed this hysteresis effect was caused mainly by the closing of a noticeable (~1/8 inch) gap between the base of

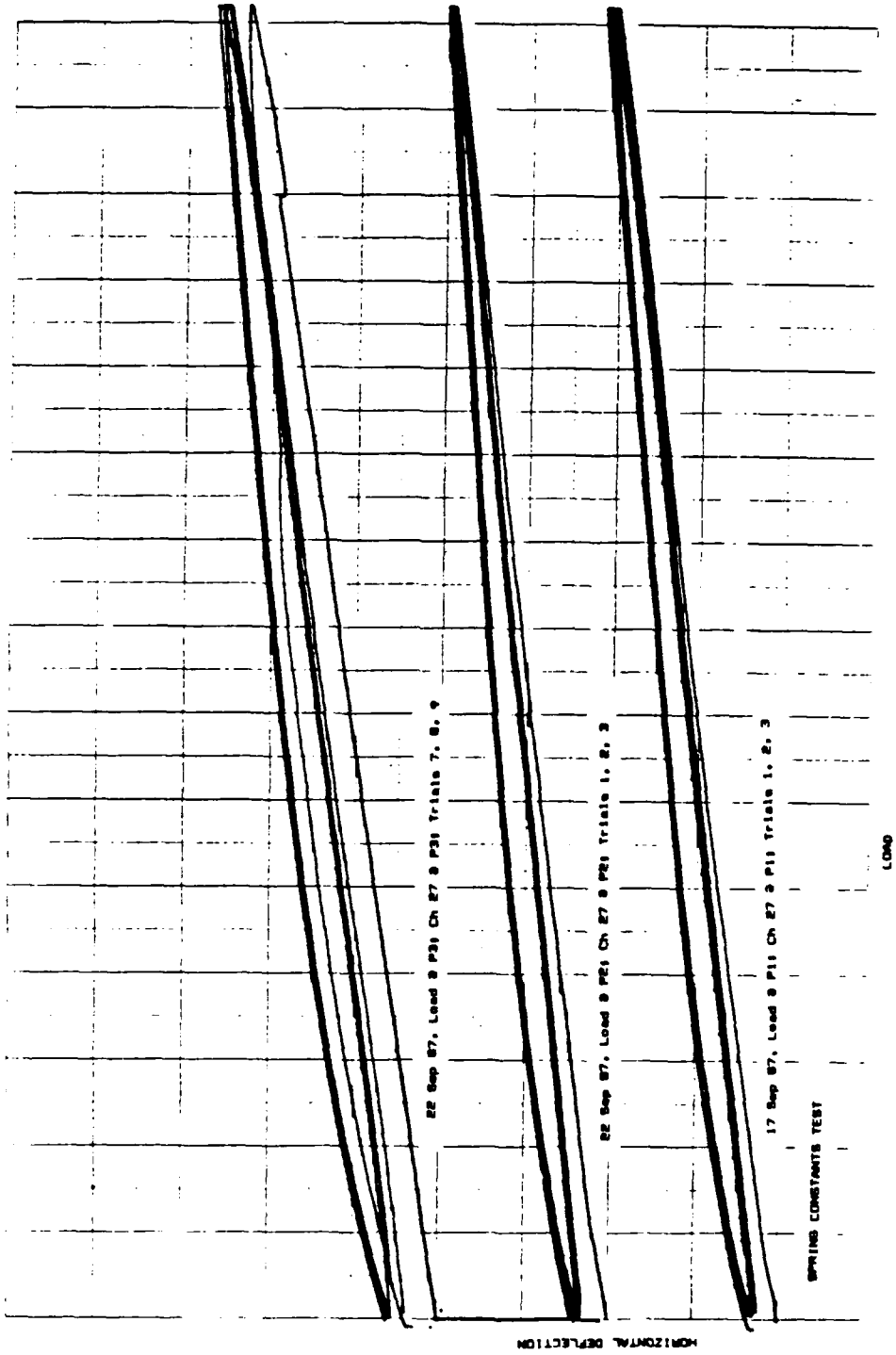


Figure 2.4 Load-Deflection Hysteresis Effect

each post and the deck when each post was loaded. The gaps evidently existed from the time of fabrication. The curb block, to which each post is bolted, extends slightly over the edge of the deck. This allows a gap between the outer deck member and the base of the posts. Also, some minute slippage of the mechanical connections was probably occurring. Perhaps even some permanent deformations of drive spikes or deck laminates was caused by the first load cycle each time. Generally, after two or three cycles, the load-deflection curve stabilized.

To determine the spring constant for each post, four load-deflection data points were chosen, usually those at 0, 1, 2, and 3 kips of load. These data points were entered into a computer program which performed a linear regression curve fit (26). The program produced the slope of the best straight line through the data points (in kips of load per

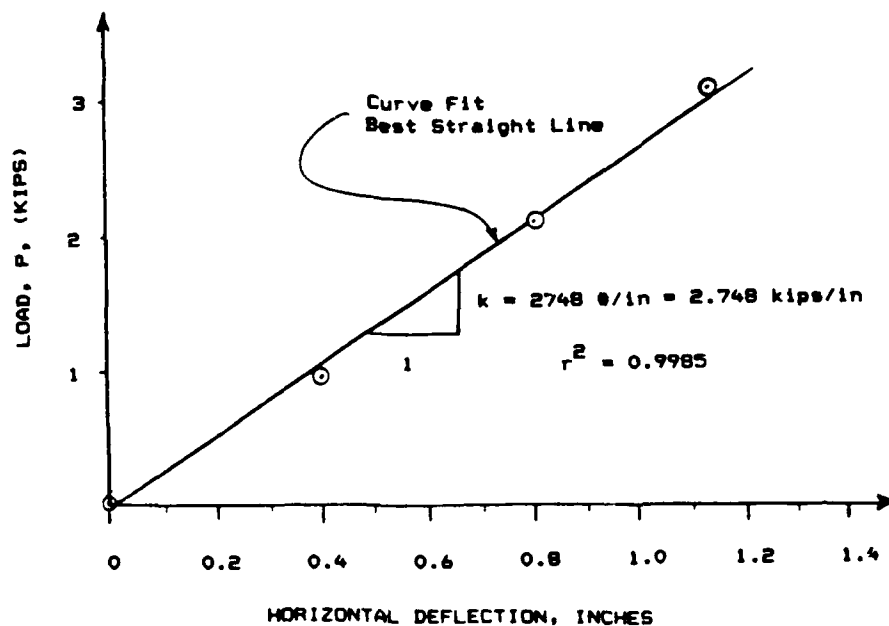


Figure 2.5 Calculating Spring Constants for Posts

inch of deflection), and the coefficient of determination, r^2 , which was an indicator of how close a straight line fit the data (see Figure 2.5) .

This procedure was repeated seven times for each post. The first load cycle for each post was discarded because of the closure between the deck and the base of the post. This resulted in a larger deflection of the post for the first trial than for subsequent trials. The remaining seven k -values were then averaged to obtain a single k -value for each of the three accessible posts. Overall, each post in each trial exhibited highly linear behavior. Table 2.1 summarizes the k -values and r^2 values, and gives the mean, \bar{x} , standard deviation, s , and coefficient of variation (COV) values for each post.

As shown in Table 2.1, the end post had a k -value of 2572 lb/in. The quarter post had a 2657 lb/in. k -value, and the center post had a 2047 lb/in. k -value. These values indicate that the center post was the most flexible. This result is understandable because under load, not only did the center post rotate about its connection to the deck, but also the deck members themselves deflected laterally when the post was loaded (see Figure 2.6). At the ends the tiedown to the strong floor through the cap greatly restrained the lateral deflection of the deck. Consequently, the deck deflected laterally much like a simple supported deep beam.

Table 2.1 Summary of Spring Constants for Rail Posts

Trial	End Post		Quarter Post		Center Post	
	k(lb/in.)	r ²	k(lb/in.)	r ²	k(lb/in.)	r ²
1*	2537	.9987	2596	.9996	1967	.9998
2	--	--	2602	.9989	2028	.9994
3	2549	.9983	2632	.9997	2040	.9995
4	2550	.9982	2690	.9988	2041	.9995
5	2561	.9981	2684	.9990	2054	.9997
6	2616	.9980	2748	.9985	2041	.9989
7	2557	.9978	2625	.9996	2064	.9996
8	2599	.9969	2619	.9991	2064	.9998

* Trial 1 results not included in statistical measure.

x :	2572 lb/in.	2657 lb/in.	2047 lb/in.
s :	28.4 lb/in.	52.0 lb/in.	13.6 lb/in.
COV :	0.0110	0.0196	0.0066

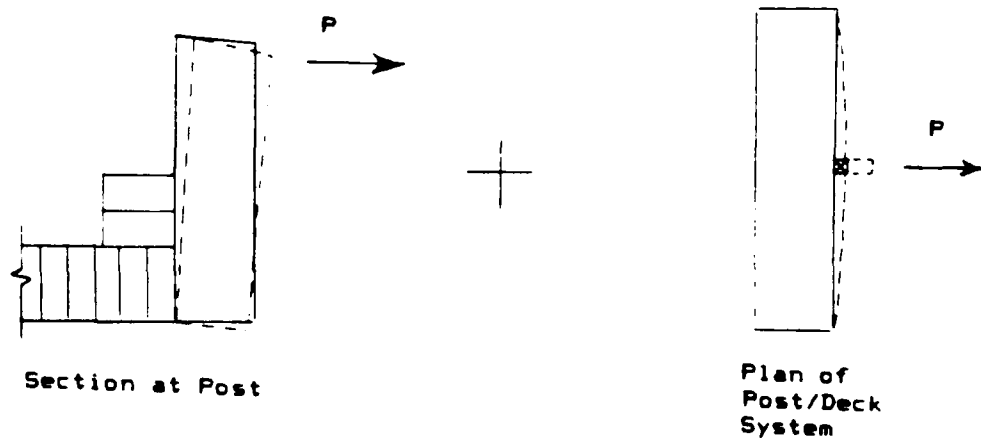


Figure 2.6 Components of Center Post Deflections

The end post was the next most flexible, but only slightly so, relative to the quarter post probably because it was very close to the end of the deck members. This allowed a large rotation of the deck members (and thus the post) under load. But the deck members could not deflect much laterally because they were close to a pile cap support (see Figure 2.7). The quarter post, located between these two extremes, exhibited the stiffest behavior. While some rational reasoning has been given for the differing flexibility coefficients, the variability associated with the post base to deck connection is likely the key factor. The physical aspect of making this connection via drive spikes is not easily controlled so as to have replication of result at each post.

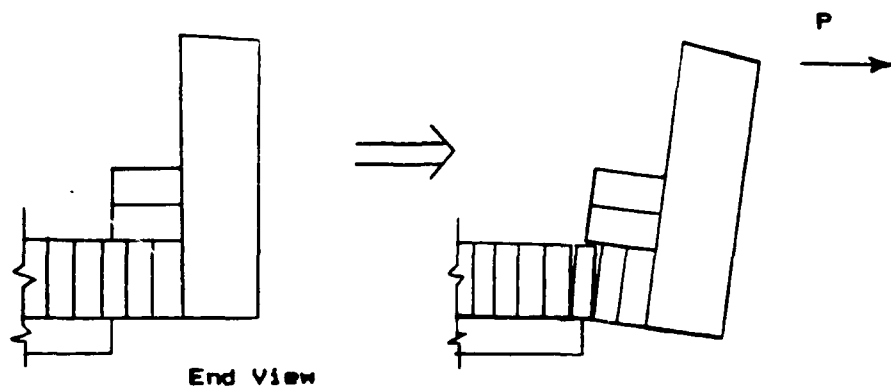


Figure 2.7 End Post Deflection

As stated before, the k -values for the two northernmost posts were obtained by assuming structural symmetry and simply using the corresponding k -values for the southernmost

two posts. All five k-values were then utilized in the matrix structural analysis of the model.

2.3 Matrix Structural Analysis Predictions (GTSTRUDL)

Once the spring constant for each post was determined, a matrix structural analysis of the model was performed to predict deflections of the timber rail system under load. This analysis was accomplished using the computer program GTSTRUDL on CSU's Control Data Corporation (CDC) Cyber 180 mainframe computer.

GTSTRUDL is a problem oriented language (POL) program which performs stiffness analyses of structures. The name, GTSTRUDL, is an acronym for Georgia Tech's Structural Design Language. The original STRUDL program was developed at the Massachusetts Institute of Technology (MIT) in the early 1960's. Georgia Institute of Technology (Georgia Tech) modified and extended it for commercial applications on CDC and VAX computers (23).

2.3.1 Model Geometry and Loads

The model geometry was entered into GTSTRUDL via an input data file. The input parameters include joint members and locations, member numbers and incidences, support conditions, material properties, and other problem descriptors. Appendix B is an echo of the input data file. Figure 2.8 is a schematic of the GTSTRUDL model of the guardrail system.

Note that the spring constants were input as support conditions, and that each spring was considered independent

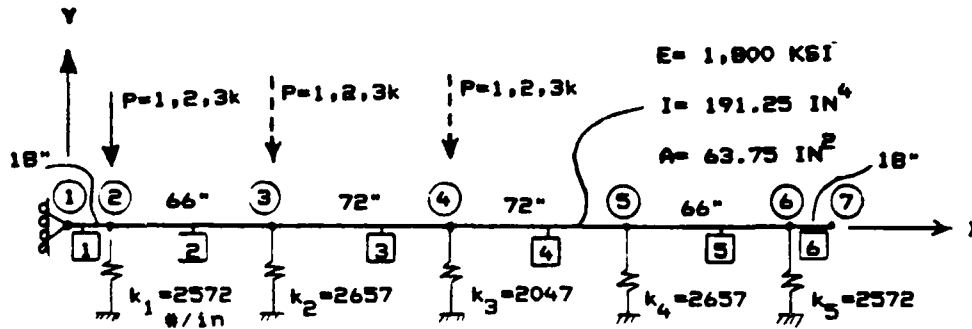


Figure 2.8 Schematic of GTSTRUDL Timber Rail Model

of the others. The pinned roller on the left end of the beam was necessary to provide structural stability to the GTSTRUDL model in the X direction. Since the loads were all perpendicular to the beam, this roller did not affect the rail deflections.

The rail was assigned a constant modulus of elasticity (MOE) of 1,800,000 psi, the average value, as listed in the NDS for a 24F-V4 glulam beam. This assumes the rail is homogeneous and the longitudinal MOE is constant along the length of the rail. Because the COV for a 24F-V4 glulam is considered to be 0.10 (16), the actual MOE of the rail has 90% probability of being within $\pm 296,000$ psi of 1,800,000 psi. The rail-to-post connections were modeled as being pinned by releasing the moment about the Y axis at each such joint. The actual connection detail falls

somewhere between fully fixed and purely pinned, and depends upon how torsionally stiff the post and post-to-rail connection is.

The GTSTRUDL model was utilized to study nine loadings. Loads of 1, 2, and 3 kips were applied to the rail at the end, quarter and center post locations respectively. The loads were applied one at a time and perpendicular to the rail.

2.3.2 GTSTRUDL Model Deflections

After the GTSTRUDL model geometry and loads were input, a stiffness analysis was performed by GTSTRUDL. The results of the analysis included rail joint deflections, and other response data. The joints of particular interest are those at the end, quarter and center post locations. These joint deflections for the various loadings are summarized in Table 2.2 . Generally, the GTSTRUDL rail deflected as would a theoretical beam on discrete elastic supports. For instance, for loads in the center of the beam, the deflections were symmetrical and the ends of the beam experienced deflections opposite the direction of the load (uplift). Also, for loads near the end of the rail, uplift was observed at a certain distance (somewhat less than a length $Z = 3\pi / 4\beta$) from the load.

2.4 Model Validation

Once the spring constants had been determined and a matrix structural analysis had been performed (GTSTRUDL) to predict deflections of the timber rail system, the actual

timber specimen was tested with the glulam rail in place to validate the model.

Table 2.2 Summary of GTSTRUDL Deflection Predictions

Load Location	Load (Kips)	Rail Deflections (in.) at Post Locations				
		End (P1)	Qtr (P2)	Ctr (P3)	Qtr (P4)	End (P5)
Post 1	1 K	.32	.10	-.01	-.02	-.01
	2	.64	.20	-.01	-.04	-.01
	3	.95	.30	-.02	-.06	-.02
Post 2	1 K	.10	.18	.11	.03	-.02
	2	.20	.37	.23	.06	-.04
	3	.30	.55	.34	.08	-.06
Post 3	1 K	-.01	.11	.21	.11	-.01
	2	-.01	.23	.42	.23	-.01
	3	-.02	.34	.63	.34	-.02

NOTE: Deflections positive in direction of load.

2.4.1 Test Setup and Procedure

The 24F-V4 glulam rail was reattached to the rail posts with two 5/8-inch diameter bolts at each post. The specimen remained connected to the pile caps as before. The same loading system and deflection measurement devices were used as were used during the spring constant testing of individual posts.

With the rail attached, the wire rope cable could not pass through the centroid of the bolted connection, and had to be wrapped around the rail and over the top of the post to reach the winch. Therefore the load application point at

each post for the rail test was higher than during the spring constant test. (see Figure 2.9)

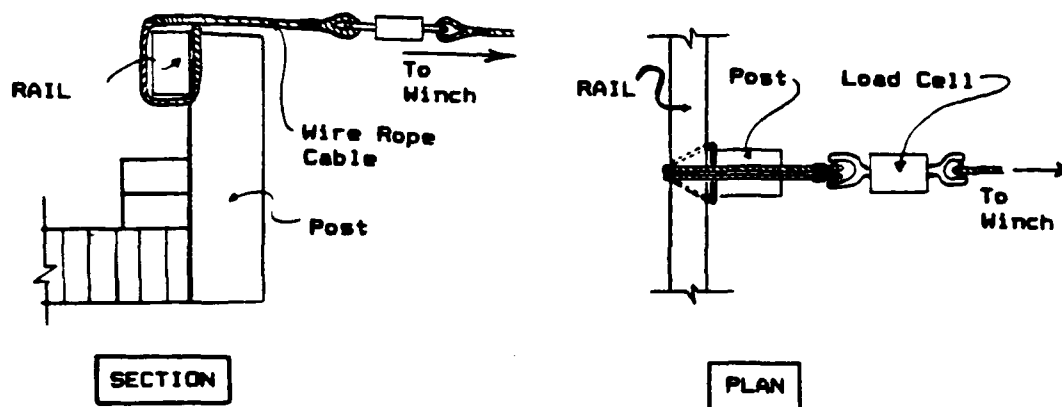


Figure 2.9 Rail Test Load Application

AASHTO requires the lateral load be applied at the centroid of the rail-to-post connection. This difference must be kept in mind when comparing the predictions of this model to not only the AASHTO requirements but also the laboratory rail test.

The rail was loaded at the accessible end, quarter, and center post locations. The load at each location was varied from 0 to 3 kips. The deflections corresponding to loads of 1, 2, and 3 kips for each post were determined by scaling the voltages recorded on the paper tape output of the data

logger. A summary of the load-deflection data are given in Table 2.3 . These load-deflection data points were compared with the GTSTRUDL predictions. Those comparisons are shown in Table 2.4 and will be discussed next.

2.4.2 Comparison of Results and Conclusions

Examination of Table 2.4 indicates that the beam on uncoupled discrete elastic supports model predicts smaller deflections than occurred from loading the actual bridge rail specimen. Figures 2.10, 2.11, and 2.12 show the displaced shape of the rail, as predicted by the model and as measured in the rail test. Quantitatively the initial model did not accurately predict the magnitudes of the deflections. Thus this model must be judged as inadequate.

The GTSTRUDL model predictions and laboratory results showed closest agreement for a 1 kip load at the center post location. This load condition produced an average 28% difference along the length of the beam. The load condition producing greatest difference was a 3 kip load at the quarter post, with an average 50% difference. By comparing individual pairs of data points, the extreme percentage differences ranged from a high of 66% to a low of 11% . These extremes occurred for a deflection at the end post due to a 1 kip load at the quarter post and for a deflection at the end post due to a 1 kip load at the end post respectively.

Table 2.3 Summary of Laboratory Rail Test Results

Rail Deflections (in.) at Post Locations										
Trl	Load	Load @ End	End Post	Qtr Ctr	Load @ Qtr	Qtr Post	End Ctr	Load @ End	End Ctr	Post Ctr
1	1 K	.40	.22	.15	.30	.27	.19	.15	.21	.27
	2	.80	.49	.37	.63	.61	.46	.34	.46	.59
	3	1.23	.77	.52	.91	.91	.70	.58	.76	1.00
2	1 K	.40	.24	.16	.28	.22	.16	.12	.17	.21
	2	.82	.52	.35	.61	.58	.43	.30	.40	.50
	3	1.23	.77	.52	.88	.89	.68	.51	.66	.85
3	1 K	.35	.22	.14	.29	.26	.19	.14	.17	.23
	2	.77	.50	.33	.60	.58	.44	.32	.42	.53
	3	1.18	.75	.50	.91	.87	.67	.51	.66	.88
4	1 K	.35	.22	.15	.29	.25	.18	.13	.17	.22
	2	.76	.49	.33	.42	.57	.43	.30	.41	.51
	3	1.18	.76	.51	.68	.86	.66	.50	.66	.88
5	1 K	.37	.24	.16	.29	.26	.19	.13	.18	.26
	2	.77	.51	.34	.59	.58	.44	.31	.39	.57
	3	1.19	.76	.50	.85	.87	.66	.52	.68	.95
6	1 K	.32	.21	.14	.28	.25	.18			
	2	.74	.48	.33	.59	.57	.42			
	3	1.16	.75	.49	.84	.86	.66			
ABORTED										
7	1 K	.35	.23	.14	.28	.22	.16	.13	.17	.27
	2	.75	.50	.33	.52	.55	.42	.31	.41	.59
	3	1.16	.75	.50	.79	.84	.65	.50	.65	.91
8	1 K	.34	.22	.15	.28	.23	.17	.14	.18	.27
	2	.75	.49	.33	.61	.55	.42	.32	.42	.59
	3	1.18	.74	.50	.87	.85	.65	.50	.65	.92
Mean	1 K	.36	.22	.15	.29	.25	.18	.13	.18	.25
	2	.77	.50	.34	.57	.57	.43	.31	.42	.55
	3	1.19	.76	.50	.84	.87	.67	.52	.67	.91

NOTE: All deflections were in the direction of the load.

Table 2.4 Comparison of Rail Test Results with GTSTRU DL Predictions

Load Location	Load	Source	Rail Deflections (in.) at Post Locations		
			End	Quarter	Center
End Post	1K	GTSTRU DL	0.32	0.10	-.01
		LAB	.36	.22	.15
	2K	GTSTRU DL	.64	.20	-.01
LAB		.77	.50	.34	
Qtr Post	1K	GTSTRU DL	.10	.18	.11
		LAB	.29	.25	.18
	2K	GTSTRU DL	.20	.37	.23
LAB		.57	.57	.43	
Ctr Post	1K	GTSTRU DL	.30	.55	.34
		LAB	.84	.87	.67
	2K	GTSTRU DL	-.01	.23	.41
LAB		.31	.42	.55	
Ctr Post	3K	GTSTRU DL	-.02	.34	.63
		LAB	.52	.67	.91

NOTE: Deflections positive in direction of load

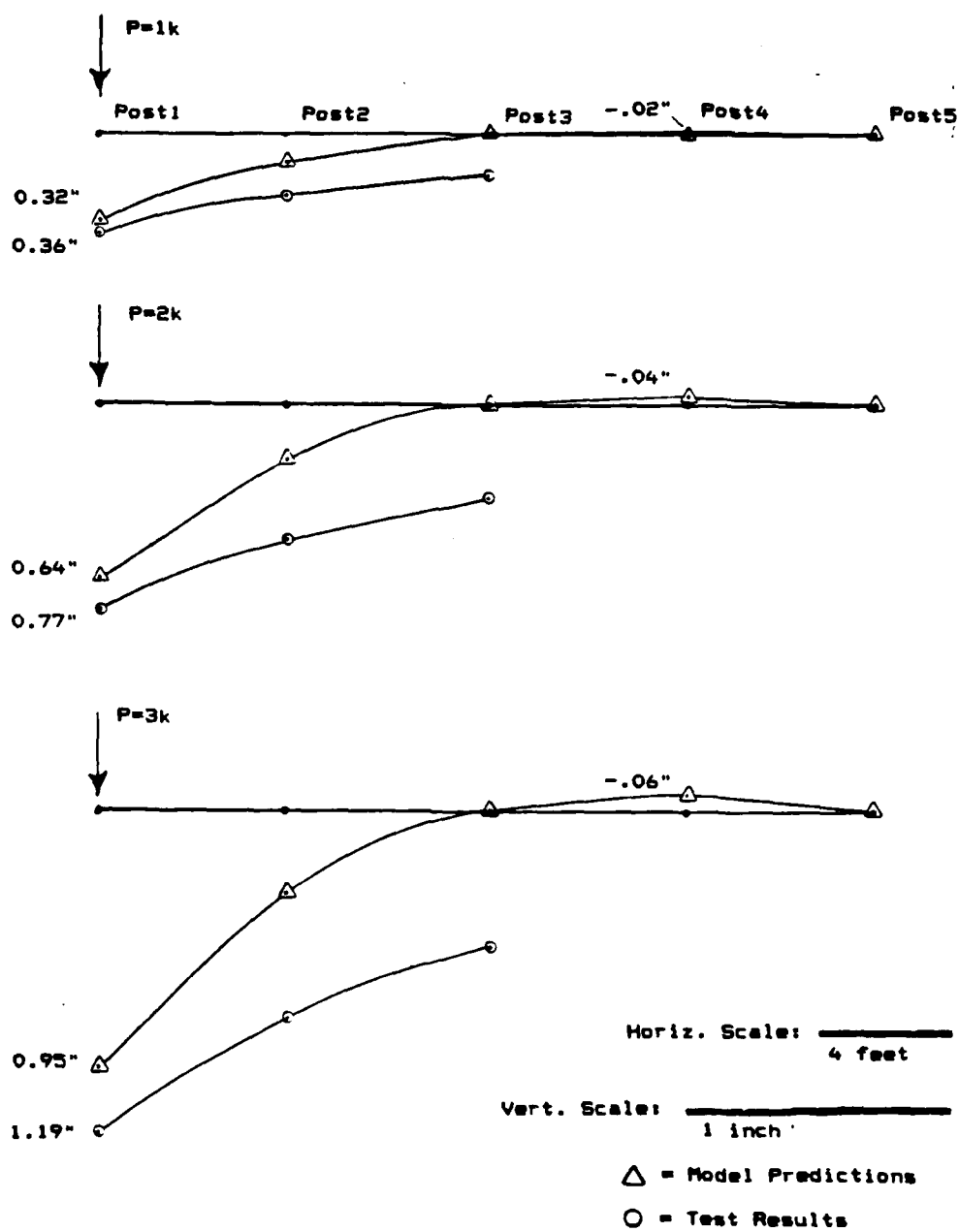


Figure 2.10 Comparison of Rail Test Results with GTSTRUDL Predictions for Load at Post 1

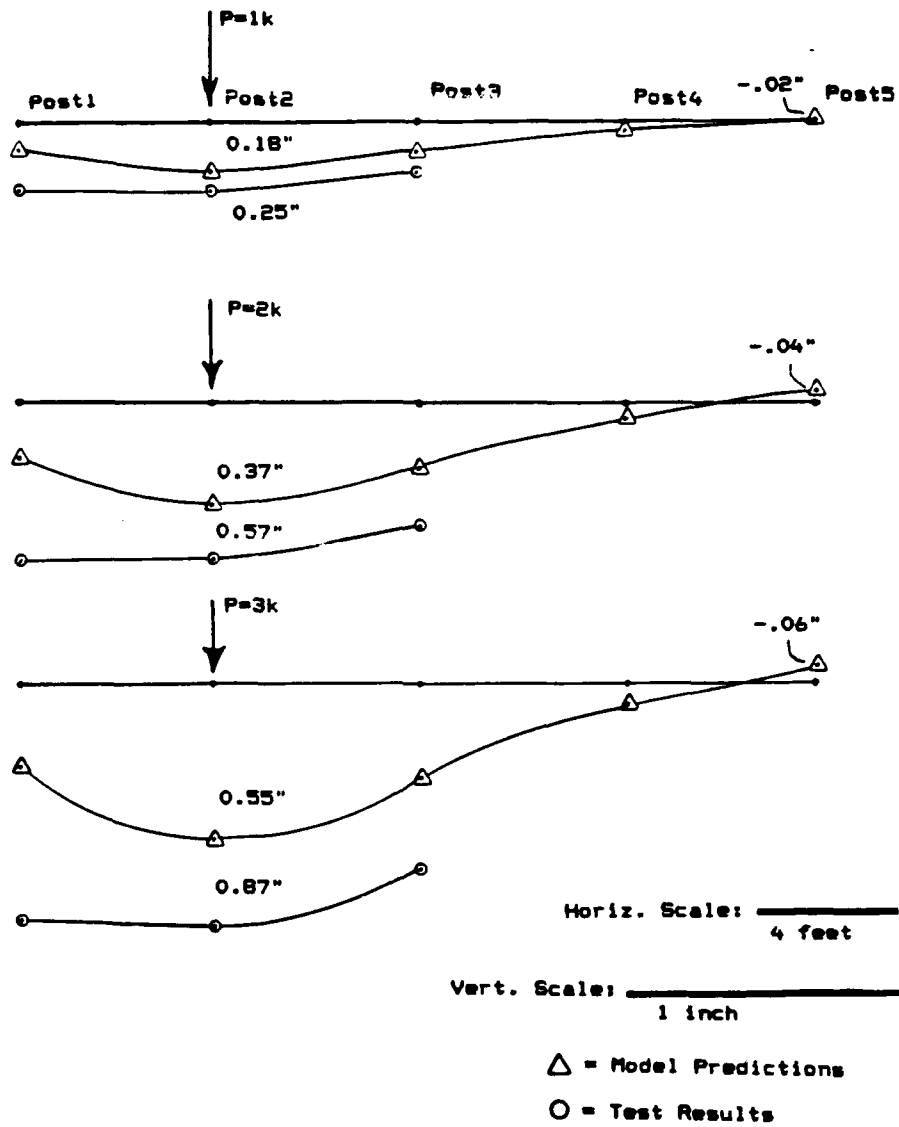


Figure 2.11 Comparison of Rail Test Results with GTSTRUDL Predictions for Load at Post 2

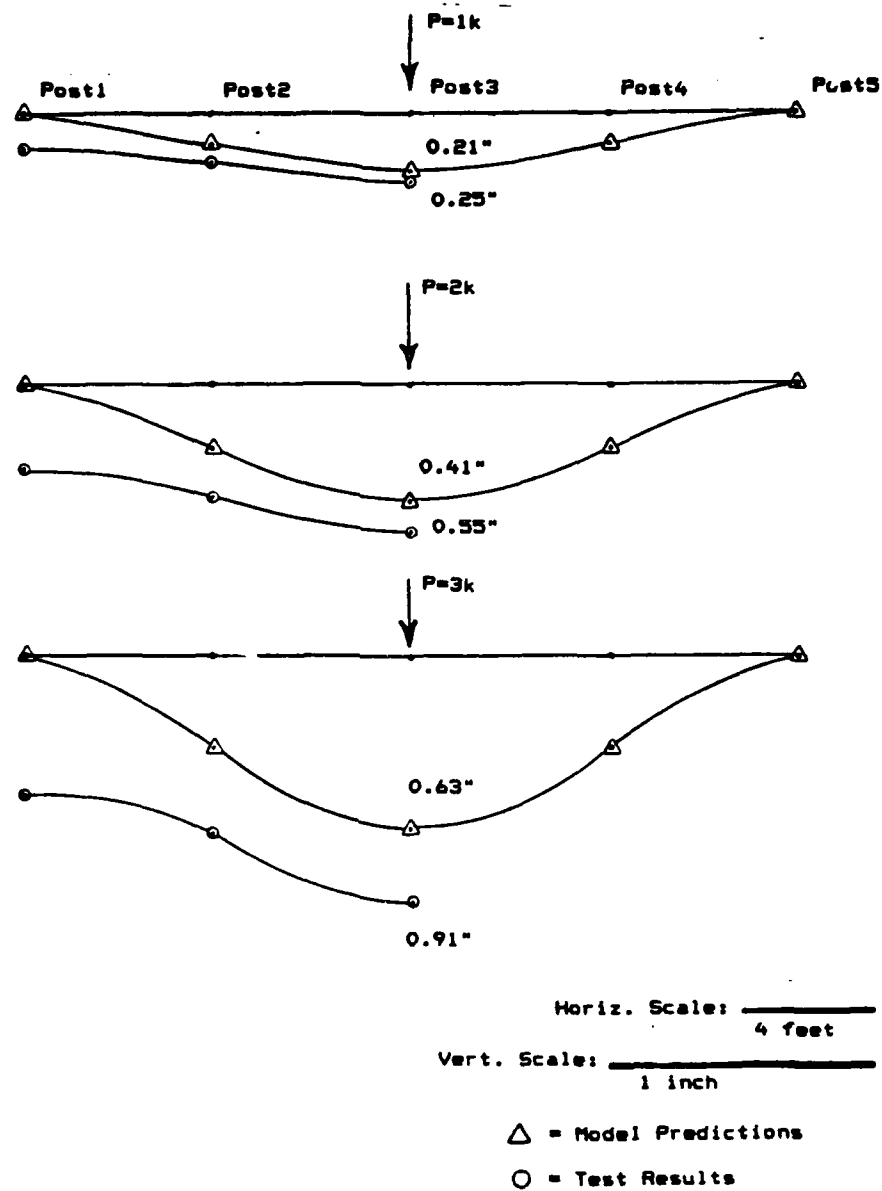


Figure 2.12 Comparison of Rail Test Results with GTSTRU DL Predictions for Load at Post 3

To assign a single value of percent difference between the GTSTRU DL model predictions and the rail test results, the percent differences for 1, 2, and 3 kip loads at the center post location were averaged. For the initial model this representative percent difference was 34%. In the preceding discussion, percent differences between very small deflections were not included in the averages.

Based on visual observations during testing, the simplifying assumption of the rail posts acting as independent springs was expected to result in some error. During the spring constant test in which one post was loaded and deflected, other posts were observed to also deflect noticeably. The rail posts are attached directly to the continuous longitudinal laminated deck and to the curb block. Apparently, when one post deflects laterally and rotates outward, the twisting of outer deck members and curb block cause outward deflections at nearby posts. Therefore the rail posts do not respond independently. By assuming independent post stiffnesses, the resulting 5 x 5 stiffness matrix for the post system (without this rail) was diagonal. In contrast, the test results indicated the stiffness matrix for the post system should be full, and not diagonal.

It was decided the model should be changed to reflect the interaction of the individual post stiffnesses. How the model was changed and the results it produced are the topics of the next chapter.

Chapter 3

SIMPLE LATERAL SPRINGS MODEL - FULL STIFFNESS MATRIX

3.1 Model Description

Once it was determined that the individual guardrail posts did not act as uncoupled springs, the model was changed to reflect this finding. Instead of the rail resting on of five independent springs, the rail was modeled as being attached to the post/deck system by use of a system of 5 coupled (via attachment to the flexible deck) transverse springs. Thus, the post/deck system is mathematically modeled by the relationship

$$\begin{Bmatrix} \Delta_1 \\ \Delta_2 \\ \Delta_3 \\ \Delta_4 \\ \Delta_5 \end{Bmatrix} = \begin{bmatrix} f_{11} & f_{12} & f_{13} & f_{14} & f_{15} \\ f_{21} & f_{22} & f_{23} & f_{24} & f_{25} \\ f_{31} & f_{32} & f_{33} & f_{34} & f_{35} \\ f_{41} & f_{42} & f_{43} & f_{44} & f_{45} \\ f_{51} & f_{52} & f_{53} & f_{54} & f_{55} \end{bmatrix} \begin{Bmatrix} P_1 \\ P_2 \\ P_3 \\ P_4 \\ P_5 \end{Bmatrix} \quad (3.1)$$

in which

Δ_i = lateral deflection of post i

P_i = transverse load at post i

f_{ij} = displacement at post i due to a unit load at post j

In symbolic form, Equation 3.1 can be shown as

$$\{ \Delta \} = [F_{pd}] \{ P \} \quad (3.2)$$

in which $[F_{pd}]$ is the flexibility matrix for the post/deck system. By loading each post one at a time (as before) and measuring displacements at all posts, experimental flexibility coefficients are obtained. Because unit loads would produce displacements too small for easy measurement, the load was varied from 0 to 3 kips. The flexibility coefficients were obtained from load deflection curves as described in section 3.2.2.

Because the post/deck test specimen is properly supported (in static equilibrium under load), the measured $[F_{pd}]$ is non-singular. Thus, Equation 3.2 can be converted to the corresponding stiffness relationship

$$\{P\} = [F_{pd}]^{-1} \{\Delta\} = [k_{pd}] \{\Delta\} \quad (3.3)$$

in which $[k_{pd}]$ is the stiffness matrix of the post/deck system. The rail is added to the model by combining its stiffness matrix with $[k_{pd}]$ by the conventional direct stiffness method (9). The modified model is depicted in Figure 3.1, with the member degrees of freedom indicated by arrows. The stiffness of the rail/post/deck system is then used in the matrix structural analysis to predict deflections.

3.2 Stiffness Matrix for Model

Determining the full stiffness matrix for the post/deck system involved first experimentally determining the full flexibility matrix. This was accomplished in a manner similar to that employed for the initial modeling using

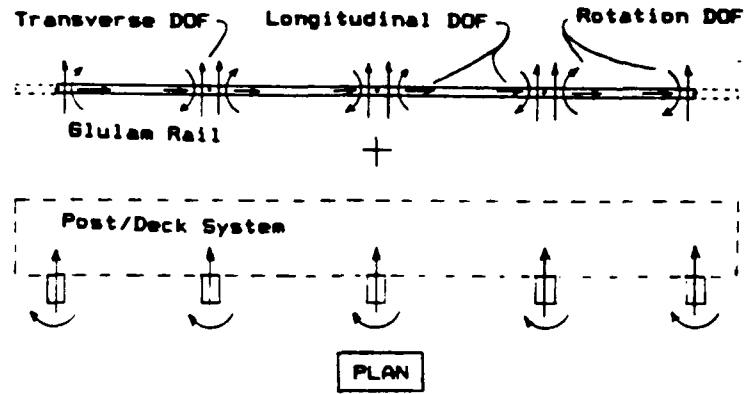


Figure 3.1 Rail on Interacting Springs Model

uncoupled springs, but additional deflection measurements were required.

3.2.1. Test Setup and Procedure

The timber bridge test specimen remained anchored to the pile caps in the same location as before. The same winch/cable loading system was used and the same DCDT's were employed. The DCDT's were recalibrated prior to the test. The guardrail was removed.

When the loads were applied to each accessible post (end, quarter, center), the deflections of the loaded post as well as the deflections of all the other posts were measured with the DCDT's. Each post was loaded once to close the gap between the deck and the base of the post, then loaded with three cycles of 0 kips to 3 kips and back

to 0 kips. This process of building the full flexibility matrix is shown schematically in Figure 3.2 .

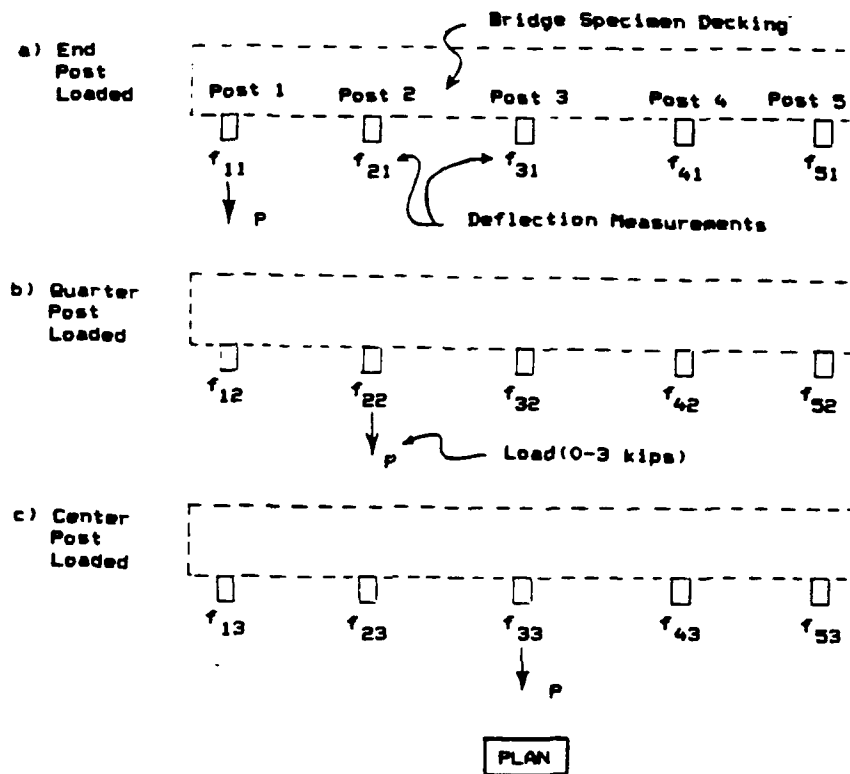


Figure 3.2 Determination of Full Flexibility Matrix for Post System

Because of the position of the test specimen, Post 4 and Post 5 could not be loaded. The flexibility matrix was therefore represented by

$$[F_{pd}] = \begin{bmatrix} f_{11} & f_{12} & f_{13} & ? & ? \\ f_{21} & f_{22} & f_{23} & ? & ? \\ f_{31} & f_{32} & f_{33} & ? & ? \\ f_{41} & f_{42} & f_{43} & ? & ? \\ f_{51} & f_{52} & f_{53} & ? & ? \end{bmatrix}$$

with direct entries for the fourth and fifth columns being unavailable. However, the geometry of the test specimen and an assumption of material, construction and connector symmetry allowed the use of a plane of symmetry through Post 3 to complete the flexibility matrix. Therefore f_{55} was assumed to equal f_{11} , f_{15} was assumed to equal f_{51} , f_{24} was assumed to equal f_{42} , etc. The resulting full flexibility matrix was represented by

$$[F_{pd}] = \begin{bmatrix} f_{11} & f_{12} & f_{13} & f_{14}=f_{52} & f_{15}=f_{51} \\ f_{21} & f_{22} & f_{23} & f_{24}=f_{42} & f_{25}=f_{41} \\ f_{31} & f_{32} & f_{33} & f_{34}=f_{32} & f_{35}=f_{31} \\ f_{41} & f_{42} & f_{43} & f_{44}=f_{22} & f_{45}=f_{21} \\ f_{51} & f_{52} & f_{53} & f_{54}=f_{12} & f_{55}=f_{11} \end{bmatrix}$$

This assumption of symmetrical measured behavior due to symmetrical geometry would be quite good for a homogeneous material with rigid connections like steel with a welded base joint. For a non-homogeneous, highly variable material like wood and for mechanical connections, the assumption is imperfect. But until the bridge test section is moved into a position where all posts could be loaded, the symmetry assumption is necessary to develop the model.

3.2.2 Reduction of Data

The number of computations required to reduce the voltage data to load and deflection data increased considerably when multiple deflections were measured for each loaded post. Therefore a simple BASIC computer program

was written to reduce the data. The listing of this program along with a sample input file and output is included in Appendix C.

To use the program, selected voltages from the data-logger paper tape were entered into a data file. The program read these voltages, computed changes in voltage (deltas), converted these deltas to loads and deflections using the appropriate calibration factors, then outputted the load-deflection data in a useable form.

These load-deflection data points were then entered into the curve-fitting program and the slope of the best straight line through the data points represented the flexibility, f_{ij} , in inches of deflection per kip of load (in/k). Five flexibilities (e.g. f_{11} , f_{21} , f_{31} , f_{41} , f_{51}) were obtained for each loaded post. The results of these measurements are presented, in a full flexibility matrix form, in Table 3.1 .

Table 3.1 Full Flexibility Matrix For Post System

$$[F_{pd}] \text{ (in/k)} = \begin{array}{ccccc|cc} .5006 & .2826 & .1471 & .0416 & .0162 & & \\ .2289 & .4514 & .2661 & .1286 & .0469 & & \\ .1094 & .2795 & .5718 & .2795 & .1094 & & \\ .0469 & .1286 & .2306 & .4514 & .2289 & & \\ .0162 & .0416 & .0950 & .2826 & .5006 & & \end{array}$$

measured reflected

3.2.3 Results

From Table 3.1 it is evident that the full flexibility matrix was close (within $\pm 15\%$ of the average of each off-diagonal pairing) to being symmetrical, even in the portion (first 3 columns) which was not a reflection. This was encouraging because a nearly symmetrical full flexibility matrix had been expected. Timber structural systems, because of the slippage of individual mechanical connections, are not likely to possess a perfectly symmetrical measured flexibility matrix.

For use in the subsequent matrix structural analysis, the flexibility matrix was adjusted such that $[F_{pd}] = [F_{pd}]^T$. Diagonal terms were retained, but each off diagonal pairing, f_{ij} and f_{ji} , was averaged, to be in accordance with the Law of Reciprocal Displacements. This adjusted flexibility matrix is shown in Table 3.2 .

With the flexibility matrix of the post/deck system having been determined, a matrix structural analysis of the rail attached to the interacting springs system (posts) was performed.

Table 3.2 Adjusted Flexibility Matrix for Post/DeckSystem

$$[F_{pd}]_{\text{adjusted}}^{(\text{in/k})} = \begin{bmatrix} .5006 & .2558 & .1282 & .0442 & .0162 \\ .2558 & .4514 & .2728 & .1286 & .0442 \\ .1282 & .2728 & .5718 & .2550 & .1022 \\ .0442 & .1286 & .2550 & .4514 & .2558 \\ .0162 & .0442 & .1022 & .2558 & .5006 \end{bmatrix}$$

3.3 Matrix Structural Analysis Predictions (Program RAIL)

3.3.1 Introduction

The computer program used to perform the matrix structural analysis of the second model was Program RAIL. Program RAIL is a modification of a simple rigid frame analysis program which uses the direct stiffness method of structure stiffness matrix construction. Program RAIL was updated to FORTRAN 77 language for this project and changed to allow the inputting of additional elements directly into the structure stiffness matrix. Program RAIL utilizes matrix structural analysis equations found in reference 10. The matrix equations utilized include:

$$\begin{aligned} \{P\} &= [E] \{F\} && \text{the equilibrium equation} \\ \{\Delta\} &= [C] \{X\} && \text{the compatibility equation} \\ \{F\} &= [S] \{\Delta\} && \text{the material properties equation} \\ [K] &= [E] [S] [C] && \text{the structure stiffness matrix} \end{aligned}$$

where

$$\begin{aligned} \{P\} &= \text{the matrix of known loads} \\ [E] &= \text{the equilibrium matrix} \\ \{F\} &= \text{the matrix of unknown member forces} \\ \{\Delta\} &= \text{the matrix of unknown member deformations} \\ [C] &= \text{the compatibility matrix} \\ \{X\} &= \text{the matrix of unknown joint displacements} \\ [S] &= \text{the member stiffness matrix} \\ [K] &= \text{the structure stiffness matrix} \end{aligned}$$

A sample input file for Program RAIL, and a sample output product is shown in Appendix D.

For the first model, GTSTRU DL was used because GTSTRU DL allowed the inputting of independent spring constants, which was the basis for the first model. The second model, with a spring system possessing a full flexibility matrix, required a program which would allow the inputting of elements directly into the structure stiffness matrix [K]. GTSTRU DL does not allow the user this option.

3.3.2 Flexibility Matrix Inversion

To input elements directly into the structure stiffness matrix of Program RAIL, the full flexibility matrix had to be converted to a stiffness matrix. This conversion was accomplished by taking the inverse of the flexibility matrix, as described earlier.

The matrix algebra computer program Symbolic Matrix Interpretive System (SMIS) (24) was used to find the inverse of the flexibility matrix. The results are shown in Table 3.3. These values were used as input to Program RAIL.

3.3.3 Model Geometry and Loads

The model geometry, along with the structure degrees of freedom, are displayed in Figure 3.3 .

Table 3.3 Full Stiffness Matrix for Post System

$$[K_{pd}] \text{ (k/in)} = \begin{bmatrix} 2.833 & -1.721 & 0.116 & 0.178 & -0.054 \\ -1.721 & 4.162 & -1.521 & -0.221 & 0.112 \\ 0.116 & -1.521 & 3.046 & -1.436 & 0.243 \\ 0.178 & -0.221 & -1.436 & 4.079 & -1.778 \\ -0.054 & 0.112 & 0.243 & -1.778 & 2.848 \end{bmatrix}$$

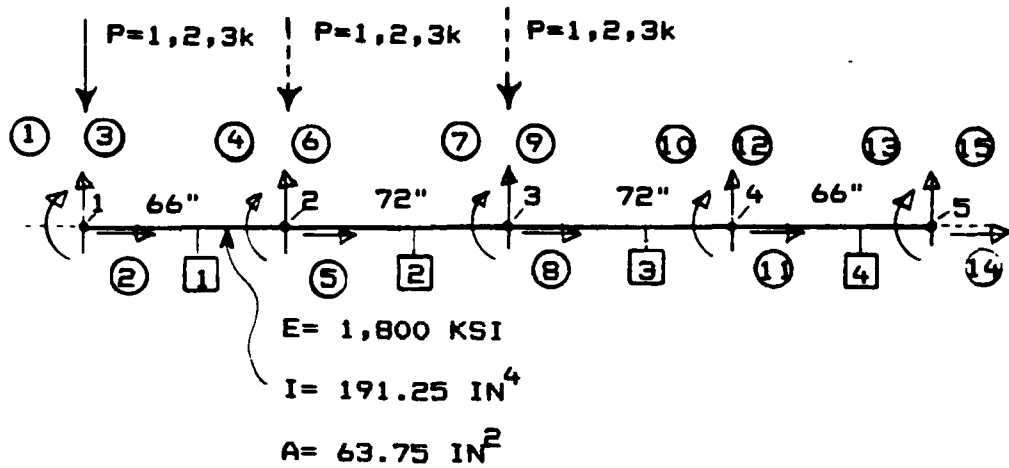


Figure 3.3 Schematic of Program RAIL Timber Rail Model

The reader should remember that the stiffness model employed in Program RAIL consists of a structure stiffness matrix assembled from the stiffness matrix of the rail itself plus the stiffness matrix of the post/deck system (represented by coupled springs). For the matrix structural analysis, the rail model was loaded at each accessible post location, one post at a time, with loads of 1, 2, and 3 kips. Loads were perpendicular to the rail. Program RAIL then was used for each load location and magnitude to perform a stiffness analysis to compute the lateral deflection of the rail at each post location. These predictions, as output from Program RAIL, are summarized in Table 3.4 .

Table 3.4 Summary of Program RAIL Deflection Predictions

Load Location	Load (Kips)	Rail Deflections (in.) at Post Locations				
		End (P1)	Qtr (P2)	Ctr (P3)	Qtr (P4)	End (P5)
Post 1	1 K	0.48	0.29	0.14	0.05	0.005
	2	.97	.57	.28	.11	.01
	3	1.45	.86	.42	.16	.01
Post 2	1 K	.29	.36	.28	.15	.05
	2	.57	.72	.57	.30	.10
	3	.86	1.09	.85	.46	.15
Post 3	1 K	.14	.28	.39	.28	.13
	2	.28	.57	.78	.56	.26
	3	.42	.85	1.16	.83	.39

NOTE: Deflections positive in direction of load. Since RAIL is based on linear, elastic behavior, the 2K and 3K results are simply multiples of the 1K results.

3.4 Model Validation

3.4.1 Rail Test Setup and Procedure

The rail was reinstalled on the timber bridge specimen, and another load-deflection test was performed to attempt to validate the second model. The specimen location, loading devices, and deflection measuring techniques were all the same as in the previous rail test.

Once again, three cycles of 0 to 3 kips loads were applied to each accessible post, and the deflections of the rail at all the posts were measured. These deflections are summarized in Tables 3.5, 3.6 and 3.7. Unfortunately, during the conduct of the rail test with the load at the quarter post, the DCDT measuring deflections at the end post malfunctioned, so those deflections are reported as missing

(MSG). The deflections of the test specimen rail are also shown graphically in Figures 3.4 and 3.5 .

3.4.2 Comparison of Results and Conclusions

A comparison of the deflections predicted by Program RAIL and those obtained in the second laboratory rail test is given in Table 3.8 . Table 3.8 shows that the beam supported on coupled elastic springs model (Program RAIL) predicts the behavior of the timber guardrail reasonably well. Overall, the deflected shape of the rail as well as the magnitudes of the deflections for the model predictions and the test results were very much alike.

The Program RAIL model predictions and laboratory results showed closest agreement for a 2 kip load at the center post location. This load condition produced an average 10% difference along the length of the beam. The load condition resulting in the greatest difference was a 1 kip load at the end post, with an average 31% difference. By comparing individual pairs of data points, the extreme percentage differences ranged from a high of 39% to a low of 0%. Those extremes occurred for a deflection at Post 3 due to a 1 kip load at Post 1 and for a deflection at Post 5 due to a 2 kip load at Post 3 respectively.

To assign a single value of percent difference between the Program RAIL model predictions and the rail test results, the percent differences for 1, 2, and 3 kip loads at the center post location were averaged, as was done for the GTSTRUDL model. For the Program RAIL model this

Table 3.5 Summary of Laboratory Rail Test Results for
Load at End Post (Post 1)

Load Location	Trl	Load (Kips)	Rail Deflections(in.) @ Post Locations				
			End (P1)	Qtr (P2)	Ctr (P3)	Qtr (P4)	End (P5)
Post 1 (P1)	1	1 K	0.67	0.43	0.23		
		2	1.17	.78	.43		
		3	1.77	1.08	.63		
	2	1 K	.72	.45	.25		
		2	1.14	.73	.42		
		3	1.77	1.07	.61		
	3	1 K	.64	.39	.21		
		2	1.06	.69	.39		
		3	1.68	1.02	.58		
	4	1 K	.64			.09	.03
		2	1.14			.19	.06
		3	1.70			.28	.09
	5	1 K	.62			.06	.03
		2	1.12			.16	.06
		3	1.68			.25	.10
	6	1 K	.62			.06	.03
		2	1.11			.16	.06
		3	1.67			.24	.09
Mean	1 K	.65	.42	.23	.07	.03	
	2	1.12	.73	.41	.17	.06	
	3	1.71	1.06	.61	.26	.09	

NOTE: All deflections were in the direction of the load.

Table 3.6 Summary of Laboratory Rail Test Results for
Load at Quarter Post (Post 2)

Load Location	Trl	Load (Kips)	Rail Deflections(in.) @ Post Locations				
			End (P1)	Qtr (P2)	Ctr (P3)	Qtr (P4)	End (P5)
Post 2 (P2)	1	1 K	MSG	0.44	0.30		
		2	MSG	.84	.62		
		3	MSG	1.19	.96		
	2	1 K	MSG	.46	.32		
		2	MSG	.85	.63		
		3	MSG	1.20	.97		
	3	1 K	MSG	.42	.29		
		2	MSG	.79	.59		
		3	MSG	1.12	.89		
	4	1 K		.50		.20	.07
		2		.90		.38	.15
		3		1.25		.56	.24
	5	1 K		.45		.15	.06
		2		.83		.32	.14
		3		1.18		.51	.22
	6	1 K		.45		.13	.05
		2		.83		.32	.13
		3		1.18		.49	.22
Mean	1 K	MSG	.45	.30	.16	.06	
	2	MSG	.84	.61	.34	.14	
	3	MSG	1.19	.94	.52	.23	

NOTE: All deflections were in the direction of the load.
MSG indicates missing data.

Table 3.7 Summary of Laboratory Rail Test Results for
Load at Center Post (Post 3)

Load Location	Trl	Load (Kips)	Rail Deflections(in.) @ Post Locations				
			End (P1)	Qtr (P2)	Ctr (P3)	Qtr (P4)	End (P5)
Post 3 (P3)	1	1 K			0.40	0.22	0.11
		2			.79	.49	.26
		3			1.16	.76	.42
	2	1 K			.40	.22	.10
		2			.80	.49	.25
		3			1.17	.77	.42
	3	1 K			.41	.22	.10
		2			.80	.50	.26
		3			1.18	.78	.41
	4	1 K	.20	.30	.42		
		2	.42	.62	.80		
		3	.63	.92	1.17		
	5	1 K	.19	.29	.40		
		2	.41	.59	.79		
		3	.63	.90	1.17		
	6	1 K	.18	.28	.39		
		2	.40	.57	.77		
		3	.61	.88	1.15		
Mean	1 K	.19	.29	.40	.22	.10	
	2	.41	.59	.79	.49	.26	
	3	.62	.90	1.17	.77	.42	

NOTE: All deflections were in the direction of the load.

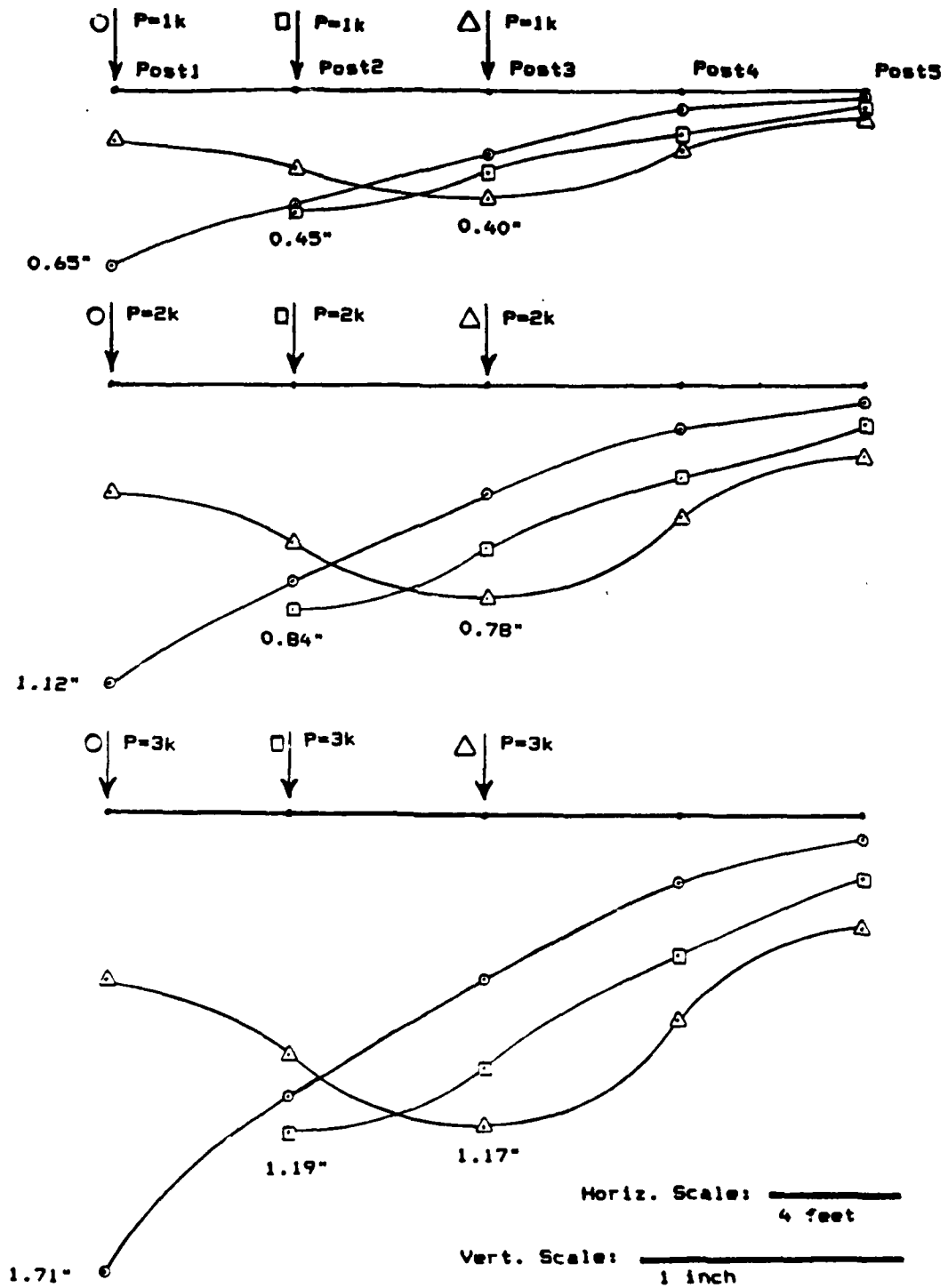


Figure 3.4 Effect of Load Position on Deflected Shape of Test Specimen Rail During Laboratory Rail Test

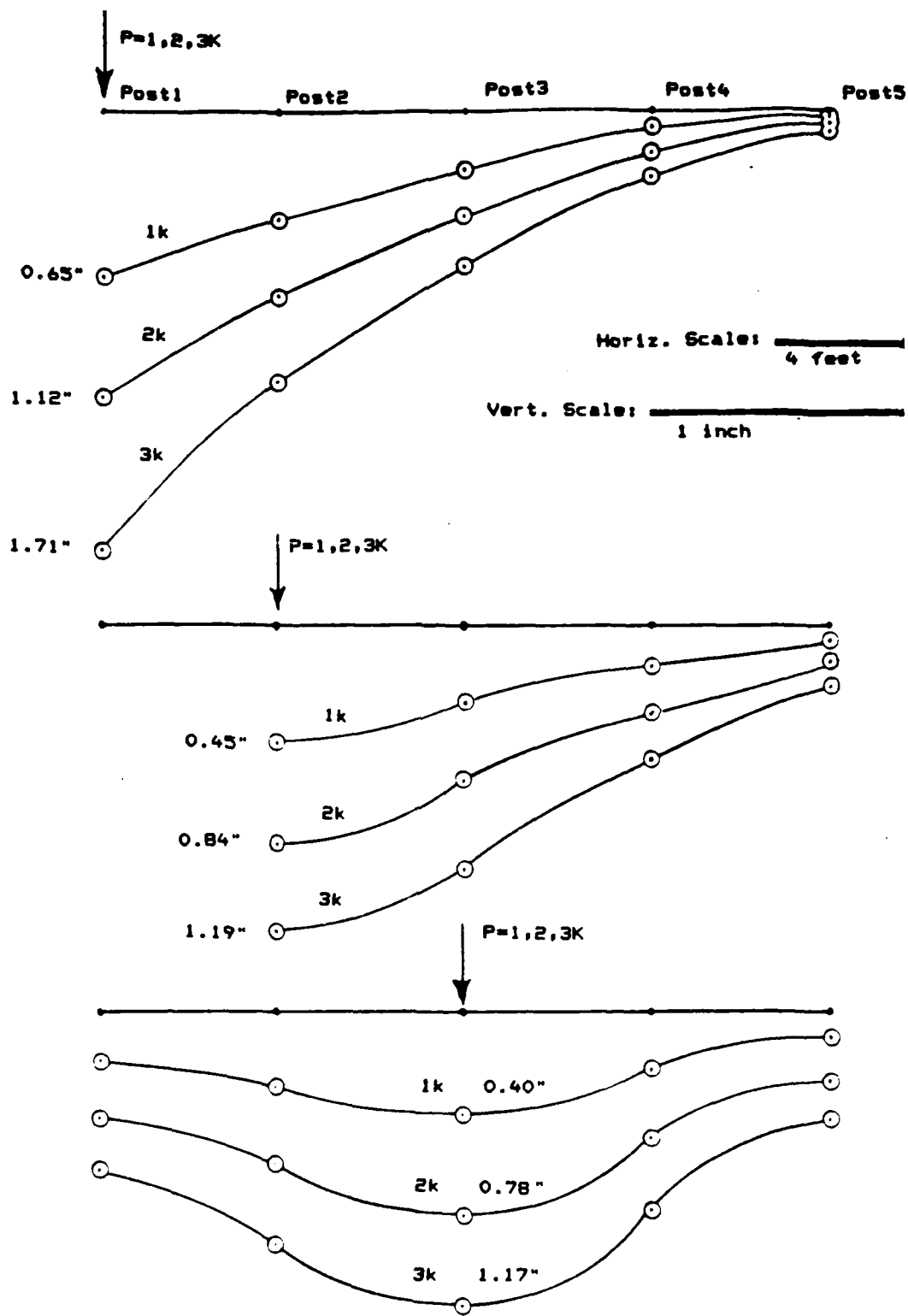


Figure 3.5 Effect of Load Magnitude on Deflected Shape of Test Specimen Rail During Laboratory Rail Test

representative percent difference was 13%. This range of error is a marked improvement over the value which resulted from the beam on uncoupled springs model. The reader will recall that for the GTSTRUDL model this representative percent difference was 34%. Again, in making this comparison, percent differences between very small deflections were not included in the averages.

The relatively good agreement of model predictions and laboratory results can be seen graphically in Figures 3.6, 3.7, and 3.8 .

The modified model produced dramatically improved results. The predicted and measured displacements of the rail were in much better agreement, both in shape and magnitude. Once again, the mathematical model generally predicted smaller deflections than the rail actually experienced in the laboratory, but the margin of difference was acceptably close.

It is possible that this difference arose for two reasons. First, the Program RAIL model received the transverse loads at the centroid of the rail, whereas the test specimen received the transverse loads across the top of the rail (see Figures 2.9 and 3.9). This 5.3 inch eccentricity of load increased the moment arm of the lateral load about the base of the loaded post. This produced a greater outward-rotating moment on the post. The eccentricity of load also imparted extra outward-rotating torsion to the rail. In the future, the individual posts

Table 3.8 Comparison of Rail Test Results with Program RAIL Predictions

Load Location	Load	Source	Rail Deflections (in.) at Post Locations				
			P1	P2	P3	P4	P5
End Post (P1)	1K	RAIL	0.48	0.29	0.14	0.05	0.005
		LAB	.65	.42	.23	.07	.03
	2K	RAIL	.97	.57	.28	.11	.01
		LAB	1.12	.73	.41	.17	.06
	3K	RAIL	1.45	.86	.42	.16	.01
		LAB	1.71	1.06	.61	.26	.09
Qtr Post (P2)	1K	RAIL	.29	.36	.28	.15	.05
		LAB	MSG	.45	.30	.16	.06
	2K	RAIL	.57	.72	.57	.30	.10
		LAB	MSG	.84	.61	.34	.14
	3K	RAIL	.86	1.09	.85	.46	.15
		LAB	MSG	1.19	.94	.52	.23
Ctr Post (P3)	1K	RAIL	.14	.28	.39	.28	.13
		LAB	.19	.29	.40	.22	.10
	2K	RAIL	.28	.57	.78	.56	.26
		LAB	.41	.59	.79	.49	.26
	3K	RAIL	.42	.85	1.16	.83	.39
		LAB	.62	.90	1.17	.77	.42

NOTE: Deflections positive in direction of load.
MSG indicates missing data.

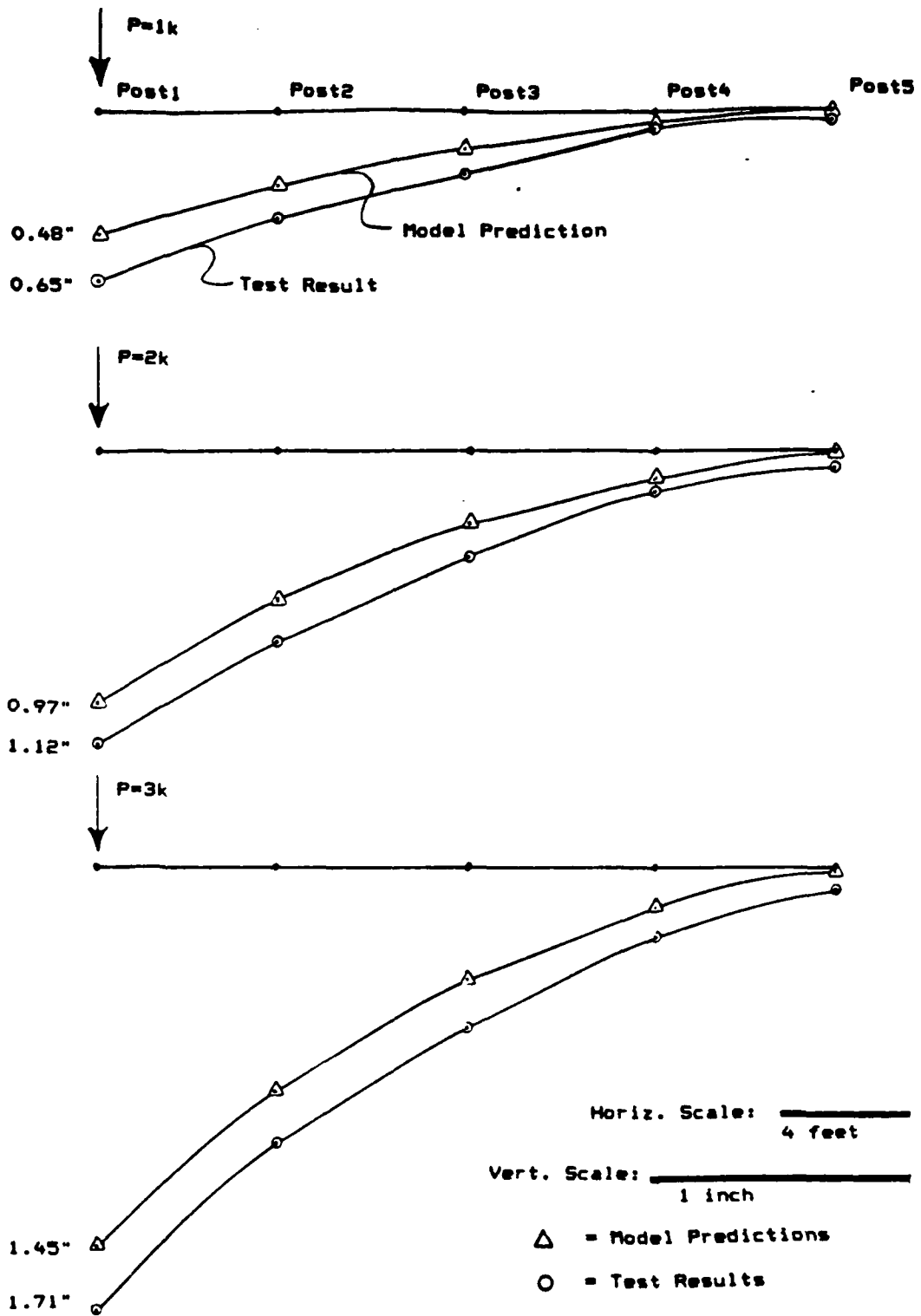


Figure 3.6 Comparison of Rail Test Results with Program RAIL Predictions for Load at Post 1

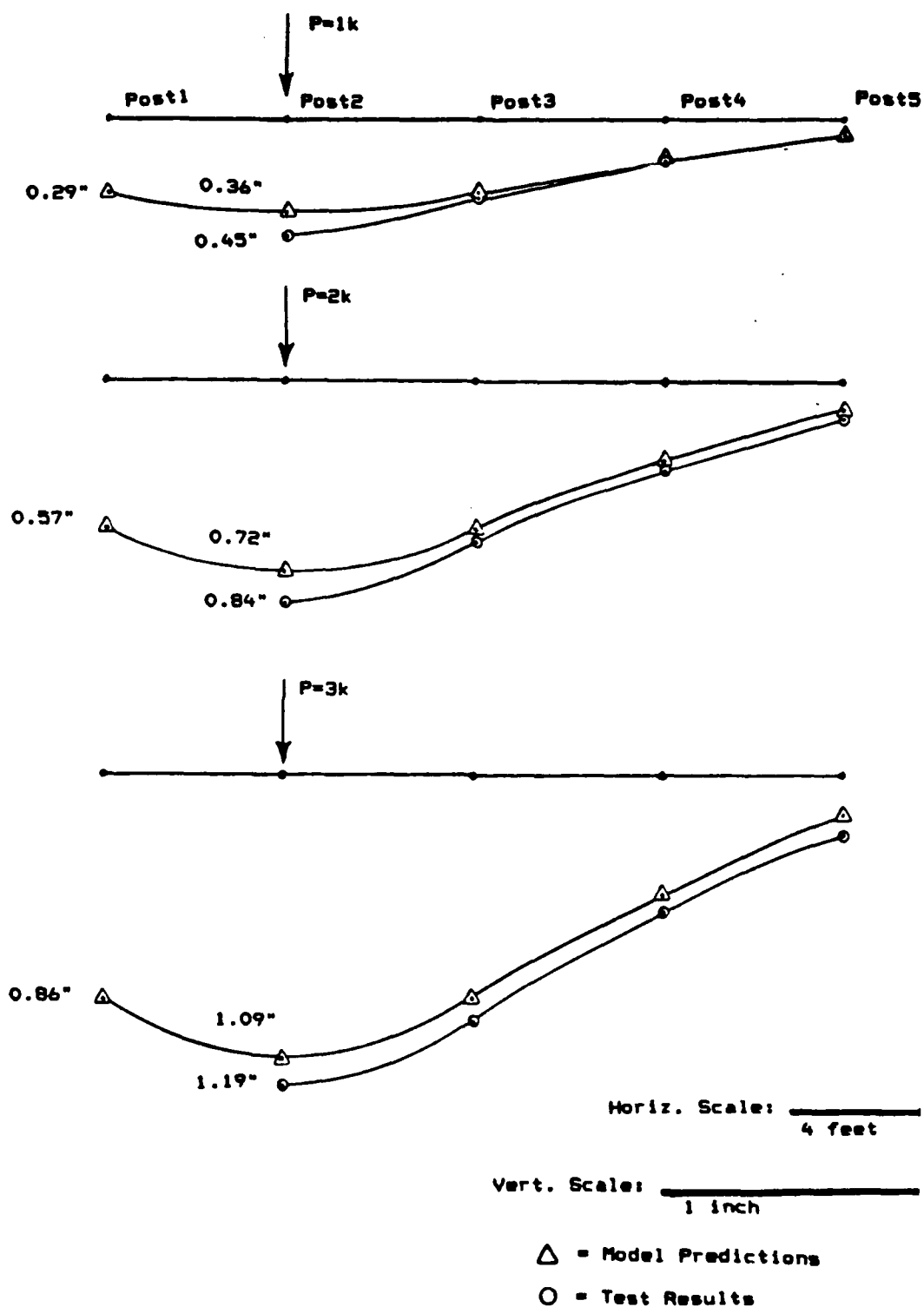


Figure 3.7 Comparison of Rail Test Results with Program RAIL Predictions for Load at Post 2

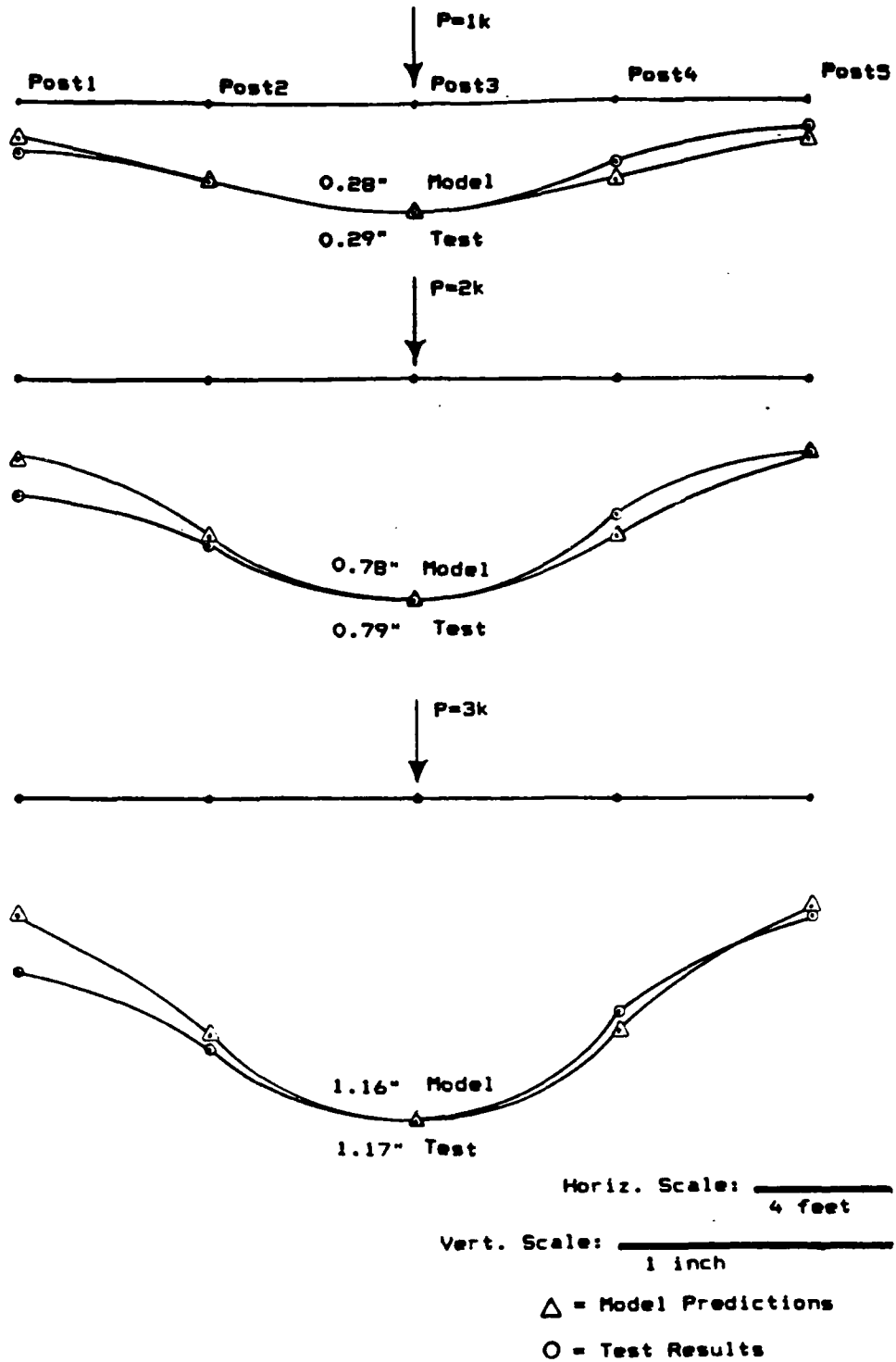


Figure 3.8 Comparison of Rail Test Results with Program RAIL Predictions for Load at Post 3

and the rail will all be loaded at the centroid of the rail-to-post connection, thus eliminating this eccentricity of load.

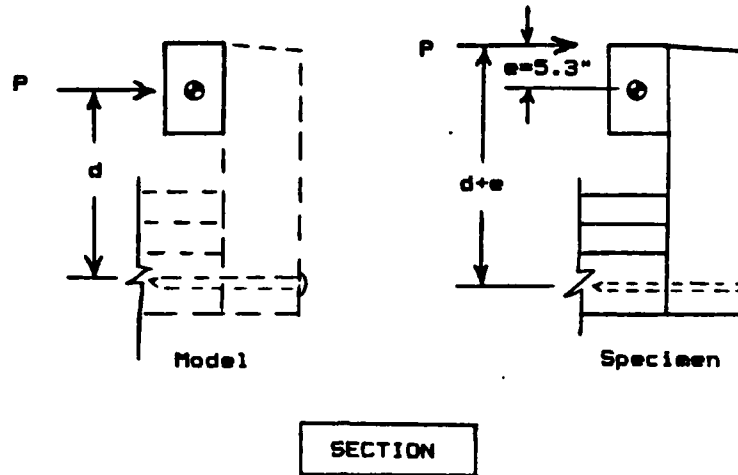


Figure 3.9 Increase in Moment Arm of Lateral Load About Base of Post

Secondly, the relative torsional resistance of the outer deck members is reduced when the guardrail system is loaded with the rail in place as opposed to when individual posts are loaded without the rail. When a single post was loaded, it rotated outward through an angle, θ , and the adjacent posts rotated outward through a much smaller angle, perhaps $\theta/4$ (see Figure 3.10). The relative torsional stiffness of the deck members between the loaded post and adjacent posts was proportional to the relative change in rotation between the posts, $\theta - \theta/4 = 3\theta/4$.

When the rail was reinstalled and the same post loaded, the post rotated through an angle θ' . However, the adjacent posts rotated through a larger percentage of θ' , perhaps $\theta'/2$, due to load sharing caused by the rail. Thus

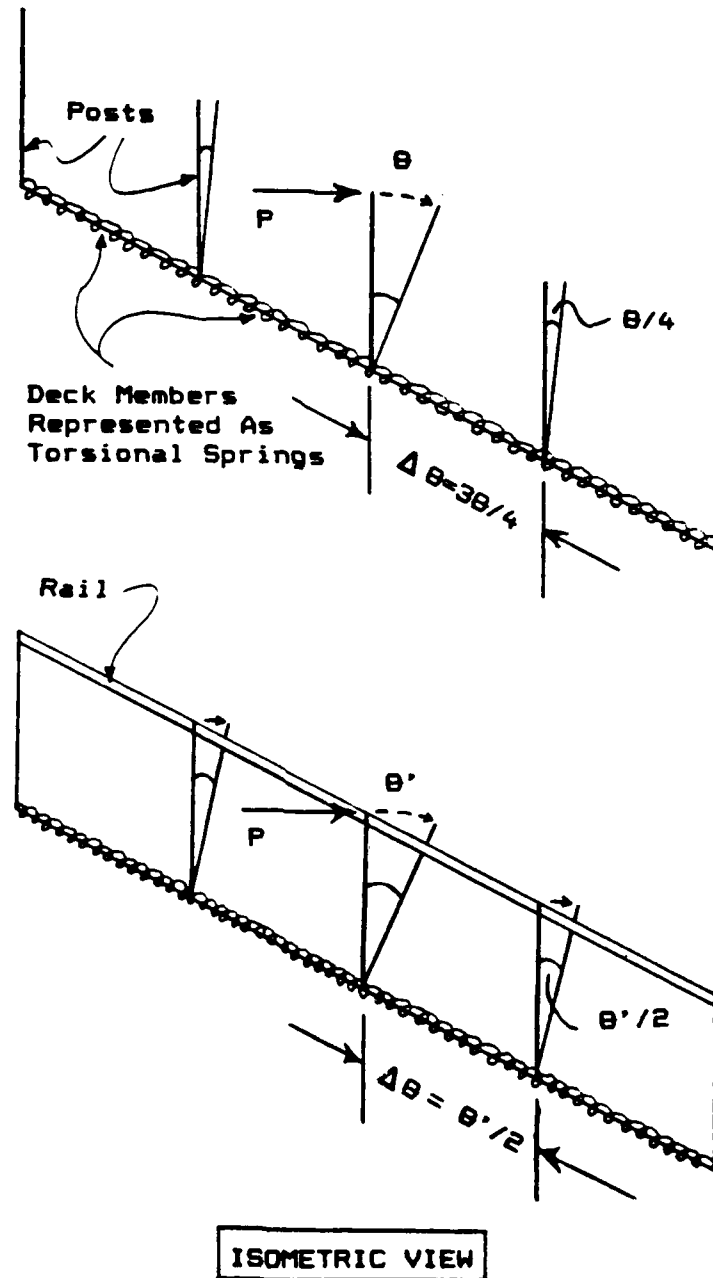


Figure 3.10 Relative Torsional Stiffness of Outer Deck Members

the relative torsional stiffness of the deck members between the loaded post and adjacent posts was proportional to a smaller relative change in rotation between the posts, $\theta' - \theta'/2 = \theta'/2$.

The effects of eccentricity of load and load sharing may have contributed to the Program RAIL model predicting slightly smaller deflections than the actual test specimen experienced under load. The use of symmetry considerations in developing the post/deck flexibility matrix also introduces some inaccuracy vis-a-vis the actual specimen.

Considering the experimental operating constraints and the necessary assumption of symmetry, this beam on coupled elastic supports model provides a reasonable way to predict the behavior of the timber bridge guardrail subjected to static loads. With some future refinements, described later, closer predictions to experimental performance can be expected to result.

3.5 Comparison of Laboratory Rail Tests

During the course of this project, two laboratory rail tests on the timber bridge specimen were performed, as previously described. A comparison of the results of these two rail tests indicated much larger deflections for the second rail test than for the first. For example, in the first rail test, a 3 kip load at the end post resulted in a rail deflection of 1.19 inches, whereas in the second rail test, the 3 kip load at the end post produced a 1.71 inch deflection.

It is believed that the difference between the two rail tests was caused by moving the specimen between tests, to accommodate testing of utility poles in another project. Between rail tests, the bridge specimen was unscrewed from the pile caps, picked up by forklifts, and moved to another location within the structures laboratory. Before the second rail test, the specimen was again pulled and lifted by forklifts and reinstalled on the pilecaps. Although as much care was taken as possible in moving the specimen, the post-to-deck connections and the deck laminates experienced dynamic loadings which may very well have loosened the connections and laminates. Also some of the rotation of the exterior deck members observed in the tests was likely altered in the lifting operation. Therefore when the second rail test was performed, it was performed on a specimen which possessed different flexibility properties.

The difference in flexibility properties can be seen by a comparison of the flexibility matrix of the post/deck system before and after moving the bridge. In the first case, the diagonal flexibility matrix of the post/deck system was given by

$$\begin{array}{l}
 [F_{pd}] \text{ (in/k)} \\
 \text{(before)}
 \end{array}
 =
 \begin{array}{c}
 \left[\begin{array}{cc}
 0.3888 & \\
 & 0.3764
 \end{array} \right] \\
 \text{measured}
 \end{array}
 \quad
 \begin{array}{c}
 \left[\begin{array}{cc}
 & 0.4885 \\
 0.3764 & \\
 & 0.3888
 \end{array} \right] \\
 \text{reflected}
 \end{array}$$

Accounting only for the diagonal terms of the full flexibility matrix, the flexibility matrix of the post/deck system after moving the specimen was given by

$$[F_{pd}] \begin{matrix} \text{(in/k)} \\ \text{(after)} \end{matrix} = \left[\begin{array}{cc|cc} 0.5006 & & & \\ & 0.4514 & & \\ & & 0.5718 & \\ & & & 0.4514 \\ & & & & 0.5006 \end{array} \right]$$

measured reflected

Averaging the five flexibilities and comparing the averages indicates a 23% increase in flexibility of the post/deck system after movement of the specimen.

For the 3 kip load condition, averaging the percent increase in the magnitude of the deflections between the two rail tests indicates a 36% increase in the magnitude of the deflections after moving the specimen.

Therefore it can be seen that moving the specimen affected the flexibility of the structure, making it more flexible, and resulting in larger deflections for the same loadings.

Moving the bridge specimen also affected the results of the two model predictions. For example, before relocating the bridge, the GTSTRUDL model predicted a 0.95 inch deflection of the rail for a 3 kip load at the end post. After shifting the bridge, the Program RAIL model predicted a 1.45 inch deflection of the rail for the same loading.

Because each model used as input the measured flexibility matrix of the post/deck specimen, the increase in flexibility of the post/deck system (due to moving the bridge) was partly responsible for causing the Program RAIL model to predict larger deflections than did the GTSTRUDL model.

3.6 Load Sharing Among Rail Posts

Based on observations of post deflections during the laboratory rail tests, it was believed that significant load sharing among the posts was occurring. To check this, the lateral post forces were computed for the nine loadings.

The post forces were computed by solving the matrix equation

$$\{F_{\text{posts}}\} = [K_{\text{pd}}] \{X_{\text{lat}}\} \quad (3.4)$$

where

$\{F_{\text{posts}}\}$ = matrix of lateral post forces

$[K_{\text{pd}}]$ = experimentally determined stiffness matrix of post/deck system

$\{X_{\text{lat}}\}$ = matrix of lateral rail deflections at post locations under load

It was found that, indeed, considerable load sharing does take place, especially when the load is not located near the end of the rail. For example, when a 1 to 3 kip load is applied to the rail at the center post location, the center post only carries 40-50 % of the total load, and the two adjacent posts carry 15-25% each. When a 1 to 3 kip load is applied at the rail at an end post location, the end post

carries 75-85% of the total load and the immediately adjacent post carries 15-20%.

Since most posts in a timber bridge railing are not end posts and terminals may be used to anchor the ends to the ground, the majority of posts in a bridge railing benefit from this load sharing effect when the rail is loaded.

Chapter 4

SUMMARY AND CONCLUSIONS

This chapter summarizes the work accomplished and the results obtained in this study, draws conclusions regarding the mathematical model as well as the timber test specimen, and makes recommendations for further study.

4.1 Summary

As stated at the beginning of this report, the purpose of this study was to create an accurate, relatively simple mathematical model of a timber bridge guardrail subjected to static loads. It was decided to model the bridge rail as a beam supported by discrete elastic springs. Two versions of this model were developed and tested.

The first model was one of a beam on uncoupled discrete spring supports. The spring constants for this model were determined experimentally using a timber bridge test specimen with the rail removed. Then the model was used to make predictions of deflection behavior with the timber rail reattached using a GTSTRUDL matrix structural analysis. Laboratory tests of the complete specimen were then conducted to examine the accuracy of the model.

The second model was a beam on coupled discrete spring supports. The full stiffness matrix of the interacting

springs (the post/deck system) was determined as the inverse of an experimentally measured flexibility matrix. The second model was used to make predictions of actual behavior using a Program RAIL matrix structural analysis. Additional rail tests in the laboratory were conducted to examine the accuracy of the second model.

The two models gave the following results. The first model (with independent springs) predicted the actual rail would behave as a theoretical beam on elastic supports, with small deflections overall and small negative deflections at locations away from the point of loading. The laboratory rail test did not validate this model. The model predicted deflections whose magnitudes only reached 34 to 89 percent of the magnitudes of the measured deflections.

The second model (with coupled springs) gave results which came considerably closer to the actual deflections. It is judged that the laboratory rail test did validate the second model. The model predicted deflections whose magnitudes ranged from 61 to 100 percent of the magnitude of the actual deflections. The highest percentages of inaccuracy were at locations where the measured displacements were small. It is an anomaly, that in such cases, small measurement errors reflect more significantly when reported as percent errors. Use of alternative instrumentations to more accurately measure the small displacements might improve the outcome.

4.2 Conclusions

The conclusions drawn from this independent study range from the general to the specific. The conclusions reached include the following:

1. A timber bridge guardrail system, statically loaded in the transverse direction, can be successfully modeled as a beam on elastic discrete coupled spring supports.

2. For the necessary modeling assumptions and experimental limitations, the RAIL model developed in this study was validated for the given load conditions. Those load conditions were 0-3 kip loads at 90 degrees to the rail at post locations. The model can be refined to include the torsional stiffnesses of the posts and the torsional stiffness of the rail.

3. In a longitudinal laminated deck (non-prestressed) timber bridge, since the rail posts are attached to the deck, there is considerable interaction of post deflections when one post is loaded. This behavior is somewhat different than "load sharing" because this behavior occurs even without the rail in place.

4. The outer two or three laminates of a longitudinally laminated deck (non-prestressed) tend to rotate outward and spread apart when the rail posts rotate outward under load. The motion likely caused the drive spikes connecting the first several laminates to experience a large amount of elastic bending when the posts rotate. Under higher loads

this spreading of the laminates and bending of the drive spikes may become excessive.

5. A longitudinal laminated deck (non-prestressed) bridge permits rather large rotations of the rail posts under static load. This is due not only to the torsional flexibility of the deck members and the bending flexibility of the drive spikes, but also to the short resisting moment arm at the post-to-deck connection.

6. When the rail of the timber bridge test specimen is loaded at the interior post locations, significant load sharing among the rail posts occurs.

7. This timber bridge guardrail modeling method, based on an experimentally determined flexibility matrix for the post/deck system, should be applicable to other superstructure configurations, provided experimental load-deflection behavior of the posts is linearly elastic, or reasonably so.

4.3 Recommendations

Although a working mathematical model of a timber bridge guardrail subjected to static loads was developed in this study, more refinement of the model is both possible and needed. It is recommended that the model be modified in the following ways:

1. Repeat the experimental determination of the flexibility matrix for the post/deck system by loading all five of the posts, one at a time, and measuring all five post deflections simultaneously.

2. Repeat the laboratory rail test, loading the rail at all five of the post locations, one at a time, and measuring all five of the rail deflections simultaneously.

3. Load the posts and the rail in both tests at the same point assumed in the structural analysis, in this case the centroid of the rail-to-post connection.

4. To be able to compare results between two different rail tests or two different models, do not move, lift, or relocate the bridge specimen between the two rail tests. The act of shifting the bridge specimen affects the flexibility properties of the specimen.

5. Measure the longitudinal stiffnesses of the posts and include these in the model.

6. Measure and accurately model the torsional stiffness of each post.

7. Include the torsional stiffness of the rail in the model.

8. Further upgrade Program RAIL to be more user friendly, to compute member shears and moments, to include graphics capability, and perhaps to make RAIL an interactive program.

9. Validate the model for greater loads, loads on the rail between two posts, and loads at an angle to the rail less than 90 degrees.

10. Model and validate the model for a timber guardrail system attached to a post-tensioned longitudinal deck bridge specimen.

Some of these suggested changes are more easily accomplished than are others. At the time of this writing, most of the recommendations are already being considered and implemented in continuing project work.

A final recommendation would be to validate the model using additional test specimens. The full stiffness matrices of these new post systems would also have to be determined experimentally. But one day, after an appropriate testing program, either an average stiffness matrix or typical stiffness matrices for a various deck, post, rail and connection configurations should be available and the model would be applicable without actually testing the bridge rail being modeled. Similar determinations could be made for other timber bridge systems, in addition to the longitudinal deck bridge.

REFERENCES

1. Arnold, A., "Bridge Deck Designs for Railing Impacts", Transportation Research Record 970, Washington, D.C., 1984.
2. Boresi, A.P., and Sidebottom, D.M., Advanced Mechanics of Materials, John Wiley and Sons, New York, NY, 1985.
3. Bronstad, M.E., and McDevitt, C.F., "Design and Development of Self-Restoring Traffic Barriers", Transportation Research Record 970, Washington, D. C., 1984.
4. Bronstad, M.E., Michie, J.D., and Mayer, J.B., Jr., "Minicar Crash Test Evaluation of Longitudinal Traffic Barrier", Transportation Research Record 1024, Washington D.C., 1985.
5. Brungraber, R.L., Gutkowski, R.M., Kindya, W., and McWilliams, R., "Timber Bridges: Part of the Solution for Rural America", Fourth International Conference on Low Volume Roads, Cornell University, Utica, N.Y., 1987.
6. Criswell, M.E., CE 560 Advanced Mechanics of Materials Class Notes, Colorado State University, Fort Collins, CO, Fall 1986.
7. Denman, O.S., and Krage, W.G., "Transitioning End Terminal -- A TREND for the Future", Effectiveness of Highway Safety Improvements, J.F. Carney III, editor, American Society of Civil Engineers, New York, NY, 1986.
8. Eslyn, W.E. and Clark, J.W., "Wood Bridges, -- Decay Inspection and Control", Agriculture Handbook 557, U.S. Forest Service, USDA, Washington, D.C., October 1979.
9. Gutkowski, R.M., "Initiatives to Reintroduce Timber Bridges in the United States", UNIDO Publication ID/WG.447/5, United Nations Industrial Development Organization, Vienna, Austria, 1985.

10. Gutkowski, R.M., Structures -- Fundamental Theory and Behavior, Van Nostrand Reinhold Company, New York, NY, 1981.
11. Hale, C.Y., "Static Load Tests of Weyerhaeuser Bridge Rail System", Weyerhaeuser Company, Seattle, WA, 1977.
12. Hetenyi, M., Beams on Elastic Foundation, University of Michigan Press, Ann Arbor, MI, 1946.
13. Hirsch, T.J., and Fairbanks, W.L., "Bridge Rail to Contain and Redirect 80,000-lb Tank Trucks", Transportation Research Record 1024, Washington D.C., 1985.
14. Metzger, R., "The Immovable Feast", Construction News Magazine. (issue unknown)
15. "Modern Timber Highway Bridges - A State of the Art Report", American Institute of Timber Construction, Englewood, CO, 1973.
16. National Design Specifications for Wood Construction, National Forest Products Association, Washington, D.C., 1982.
17. Powers, R.D., "Traffic Barriers: A Second Chance", Effectiveness of Highway Safety Improvements, J.F. Carney III, editor, American Society of Civil Engineers, New York, NY, 1986.
18. Richardson, D.B., "To Rebuild America - \$2,500,000,000 Job", U.S. News & World Report. September, 1982.
19. Roschke, P.N., and Yung, C., "Crash Performance of Vehicles Against an Energy Absorbing Bridge Guardrail", Texas Civil Engineer, December 1986.
20. Scholten, J.A., "Timber Connector Joints, Their Strengths and Designs", USDA, Technical Bulletin Number 865, Forest Products Laboratory, Madison, WI, 1944.
21. Standard Specifications for Highway Bridges, AASHTO Washington, D. C., 1983 plus 1984, 1985, 1986 Interims.
22. Timber Bridge Design, Whcelser Consolidated, Inc., Des Moines, IA.
23. Vanderbilt, M.D., CE 666 Advanced Structural Analysis Class Notes, Colorado State University, Fort Collins, CO, Fall, 1986.

24. Wilson, E.L., "SMIS -- Symbolic Matrix Interpretative System", Report No. UC SESM 73-3, Department of Civil Engineering, Berkeley, CA, 1963 revised 1973.
25. Workshop on Timber Bridge Technology Transfer, U.S. Forest Service, State and Private Forests, Milwaukee, WI, October, 1983.
26. Wong, H., BASIC Curve Fitting Program CURFIT.BAS, Waterways Experiment Station, Vicksburg, MS, 1974.

APPENDIX A

Effective Beam Length and Relative Post Spacing Calculations

EFFECTIVE LENGTH OF BEAM (RAIL)

$$L'' = m * L_s \quad \text{where } m = \text{number of springs (posts)}$$

$$L'' = 5 * 69'' \quad L_s = \text{constant spring spacing}$$

$$L'' = 345'' \quad L_s \text{ avg} = (2 * 66 + 2 * 72) / 4 = 69''$$

Compute :

$$\beta = (k/4EI)^{1/4} = \left(\frac{(3.394 \text{ kips/in.}) / (69 \text{ in.})}{(4 * 1,800 \text{ kips/in.}^2) * (191.25 \text{ in.}^4)} \right)^{1/4}$$

$$\beta = 0.01375 / \text{in.} ; 1/\beta = 72.74 \text{ in.}$$

Compute $3\pi/2\beta$:

$$3\pi/2\beta = 3/2 * \pi * 1/\beta = 3/2 * \pi * 72.74'' = 342.8'' \sim 343''$$

$$L'' > 3\pi/2\beta$$

345'' > 343'' therefore rail is "long" beam (just barely)

RELATIVE SPRING (POST) SPACING

Check $L_s \leq \pi/4\beta$:

$$L_s = 69'' \text{ (see above)} ; \quad \pi/4\beta = \pi/4 * 72.74 \text{ in.}$$

$$69'' > 57.1'' \quad \text{NG, posts are too far apart}$$

How much too far apart? $69/57 = 1.21$ or 21% .

APPENDIX B

GTSTRUDL Input File


```
$ -----
$
$ CONSTANTS
$   E   1800000.
$
$   DEFINE MEMBER SECTION PROPERTIES.
$ -----
$
$ MEMBER PROPERTIES PRISMATIC
$ 1 TO 6   AX  63.75   IZ  191.25
$
$   DEFINE STATIC TEST LOADINGS.
$ -----
$
$ LOADING 1 'CENTER POST, 1 KIP '
$   JOINT LOADS
$     4 FORCE Y -1000.
$ LOADING 2 'CENTER POST, 2 KIPS'
$   JOINT LOADS
$     4 FORCE Y -2000.
$ LOADING 3 'CENTER POST, 3 KIPS'
$   JOINT LOADS
$     4 FORCE Y -3000.
$ LOADING 4 'QTR POST, 1 KIP '
$   JOINT LOADS
$     3 FORCE Y -1000.
$ LOADING 5 'QTR POST, 2 KIPS'
$   JOINT LOADS
$     3 FORCE Y -2000.
$ LOADING 6 'QTR POST, 3 KIPS'
$   JOINT LOADS
$     3 FORCE Y -3000.
$ LOADING 7 'END POST, 1 KIP '
$   JOINT LOADS
$     2 FORCE Y -1000.
$ LOADING 8 'END POST, 2 KIPS'
$   JOINT LOADS
$     2 FORCE Y -2000.
$ LOADING 9 'END POST, 3 KIPS'
$   JOINT LOADS
$     2 FORCE Y -3000.
$
$   ECHO GEOMETRY AND LOADING DATA.
$ -----
$
$ PRINT STRUCTURAL DATA
$
$   PLOT STRUCTURE FOR GEOMETRY VERIFICATION.
$ -----
$
$ PLOT DEVICE PRINTER LENGTH 8 WIDTH 13
$ PLOT FORMAT NORMAL
$ PLOT PROJECTION Z 0.
$
```

```
$ PERFORM STIFFNESS ANALYSIS.  
$ -----  
$  
$ STIFFNESS ANALYSIS  
$  
$ LIST RESULTS OF STIFFNESS ANALYSIS.  
$ -----  
$  
$ LIST DISPLACEMENTS REACTIONS FORCES LOADS ALL  
$  
$  
$ FINISH
```

APPENDIX C

BASIC Data Reduction Routine

Program RAILDATA Listing

Sample Input Data File

Sample Output Product

PROGRAM RAILDATA LISTING

```

10  REM MARK MALONE, MASTER'S INDEPENDENT STUDY, SEPTEMBER 1987
20  REM *****
30  REM BASIC PROGRAM RAILDATA
40  REM *****
50  REM This is a data reduction routine for converting voltages
60  REM to loads and deflections. The voltages came from tests
70  REM of the timber bridge guardrail posts at the ERC.
80  REM This program reads a set of voltages from a data file
90  REM called B:DATAPOST.DAT , computes the changes in
100 REM voltage, computes the loads and deflections,
110 REM prints the results with labels, then repeats this
120 REM process as many times as the user requests.
130 REM *****
140 REM Dimension all arrays
150 REM *****
160 DIM CH30(4),CH28(4),CH27(4),CH23(4),DEL30(4),DEL28(4),
    DEL27(4),LOAD23(4)
170 REM *****
180 REM Open data file and read number of trials (i.e. # of sets
    of voltages).
190 REM *****
200 OPEN "I",#1,"B:DATAPOST.DAT"
210 INPUT#1,LABEL$
220 INPUT#1,NTRIAL%
230 PRINT "THE DATA FILE LABEL IS: ";LABEL$
240 LPRINT "THE DATA FILE LABEL IS: ";LABEL$
250 PRINT "THE NUMBER OF TRIALS IS: ";NTRIAL%
260 LPRINT "THE NUMBER OF TRIALS IS: ";NTRIAL%
270 PRINT
280 LPRINT
290 FOR I=1 TO NTRIAL%
300 PRINT "*****IN TRIAL #";I;"*****"
310 LPRINT "*****IN TRIAL #";I;"*****"
320 FOR J=1 TO 4
330 INPUT#1,CH30(J),CH28(J),CH27(J),CH23(J)
340 PRINT "FOR LOAD ";J;"VOLTAGE VALUES ARE: ";CH23(J);CH27(J);
    CH28(J);CH30(J)
350 LPRINT "FOR LOAD ";J;"VOLTAGE VALUES ARE: ";CH23(J);CH27(J);
    CH28(J);CH30(J)
360 PRINT
370 LPRINT
380 NEXT J
390 PRINT " LOAD23"," DEL27"," DEL28"," DEL30"
400 LPRINT " LOAD23"," DEL27"," DEL28"," DEL30"
410 PRINT
420 LPRINT
430 FOR K=2 TO 4
440 LET DEL30(K)=( CH30(1)-CH30(K) ) / .209
450 LET DEL28(K)=( CH28(1)-CH28(K) ) / .115
460 LET DEL27(K)=( CH27(1)-CH27(K) ) / .12
470 LET LOAD23(K)=( CH23(1)-CH23(K) ) * 10000!
480 PRINT LOAD23(K),DEL27(K),DEL28(K),DEL30(K)
490 LPRINT LOAD23(K),DEL27(K),DEL28(K),DEL30(K)
500 PRINT
510 LPRINT
520 NEXT K
530 NEXT I
540 END

```

SAMPLE INPUT DATA FILE

SPRING CONSTANT DATA FROM 17 SEP 87

2

.518	.531	.589	.384
.468	.518	.522	.276
.405	.498	.453	.170
.354	.481	.392	.083

.513	.529	.584	.370
.465	.517	.519	.272
.405	.499	.453	.173
.347	.479	.380	.072

SAMPLE OUTPUT PRODUCT

THE DATA FILE LABEL IS: SPRING CONSTANT DATA FROM 17 SEP 87
 THE NUMBER OF TRIALS IS: 2

*****IN TRIAL # 1*****

FOR LOAD 1 VOLTAGE VALUES ARE: .384 .589 .531 .518

FOR LOAD 2 VOLTAGE VALUES ARE: .276 .522 .518 .468

FOR LOAD 3 VOLTAGE VALUES ARE: .17 .453 .498 .405

FOR LOAD 4 VOLTAGE VALUES ARE: .083 .392 .481 .354

LOAD23	DEL27	DEL28	DEL30
1080	.5583331	.1130436	.2392345
2140	1.133333	.2869567	.5406699
3010	1.641667	.4347827	.784689

*****IN TRIAL # 2*****

FOR LOAD 1 VOLTAGE VALUES ARE: .37 .584 .529 .513

FOR LOAD 2 VOLTAGE VALUES ARE: .272 .519 .5170001 .465

FOR LOAD 3 VOLTAGE VALUES ARE: .173 .453 .499 .405

FOR LOAD 4 VOLTAGE VALUES ARE: .072 .38 .479 .347

LOAD23	DEL27	DEL28	DEL30
979.9999	.5416667	.1043475	.2296651
1970	1.091667	.2608693	.5167465
2980	1.7	.4347825	.7942585

APPENDIX D

Program RAIL

Sample Input Data File

Sample Output Product

SAMPLE INPUT DATA FILE

TIMBER BRIDGE RAIL, 8 DEC 87, 3K@M/S, 1K@END, 2K@QTR

15	4	3						
1801.								
1	1	2	3	4	5	6	66.	0.
63.75		191.25						
2	4	5	6	7	8	9	72.	0.
63.75		191.25						
3	7	8	9	10	11	12	72.	0.
63.75		191.25						
4	10	11	12	13	14	15	66.	0.
63.75		191.25						
2.8334		-1.7213		0.1162		0.1782		-0.0545
-1.7213		4.1621		-1.5211		-0.2213		0.1118
0.1162		-1.5211		3.0455		-1.4359		0.2425
0.1782		-0.2213		-1.4359		4.0794		-1.7776
-0.0545		0.1118		0.2425		-1.7776		2.8483
1	0.	0.		0.				
2	0.	0.		0.				
3	0.	-1.		0.				
4	0.	0.		0.				
5	0.	0.		0.				
6	0.	0.		-2.				
7	0.	0.		0.				
8	0.	0.		0.				
9	-3.	0.		0.				
10	0.	0.		0.				
11	0.	0.		0.				
12	0.	0.		0.				
13	0.	0.		0.				
14	0.	0.		0.				
15	0.	0.		0.				

SAMPLE OUTPUT PRODUCT

TIMBER BRIDGE RAIL, 8 DEC 87,LATERAL POSTS,3K0M/5,1K0END,2K00TR

MODULUS = 1801.00

DIRECT ELEMENT METHOD OF RIGID FRAME ANALYSIS

MEMBER	NP1	NP2	NP3	NP4	NP5	NP6	H	V	A	I	L	COS	SIN
1	1	2	3	4	5	6	66.0000	.0000	63.7500	191.2500	66.0000	1.00000000	.00000000

THE STIFFNESS MATRIX FOR MEMBER 1

.20875E+05	.00000E+00	-.47444E+03	.10438E+05	.00000E+00	.47444E+03
.00000E+00	.17396E+04	.00000E+00	.00000E+00	-.17396E+04	.00000E+00
-.47444E+03	.00000E+00	.14377E+02	-.47444E+03	.00000E+00	-.14377E+02
.10438E+05	.00000E+00	-.47444E+03	.20875E+05	.00000E+00	.47444E+03
.00000E+00	-.17396E+04	.00000E+00	.00000E+00	.17396E+04	.00000E+00
.47444E+03	.00000E+00	-.14377E+02	.47444E+03	.00000E+00	.14377E+02

MEMBER	NP1	NP2	NP3	NP4	NP5	NP6	H	V	A	I	L	COS	SIN
2	4	5	6	7	8	9	72.0000	.0000	63.7500	191.2500	72.0000	1.00000000	.00000000

THE STIFFNESS MATRIX FOR MEMBER 2

.19136E+05	.00000E+00	-.39866E+03	.95678E+04	.00000E+00	.39866E+03
.00000E+00	.15946E+04	.00000E+00	.00000E+00	-.15946E+04	.00000E+00
-.39866E+03	.00000E+00	.11074E+02	-.39866E+03	.00000E+00	-.11074E+02
.95678E+04	.00000E+00	-.39866E+03	.19136E+05	.00000E+00	.39866E+03
.00000E+00	-.15946E+04	.00000E+00	.00000E+00	.15946E+04	.00000E+00
.39866E+03	.00000E+00	-.11074E+02	.39866E+03	.00000E+00	.11074E+02

MEMBER	NP1	NP2	NP3	NP4	NP5	NP6	H	V	A	I	L	COS	SIN
3	7	8	9	10	11	12	72.0000	.0000	63.7500	191.2500	72.0000	1.00000000	.00000000

THE STIFFNESS MATRIX FOR MEMBER 3

```

.19136E+05 .00000E+00 -.39866E+03 .95678E+04 .00000E+00 .39866E+03
.00000E+00 .15946E+04 .00000E+00 .00000E+00 -.15946E+04 .00000E+00
-.39866E+03 .00000E+00 .11074E+02 -.39866E+03 .00000E+00 -.11074E+02
.95678E+04 .00000E+00 -.39866E+03 .19136E+05 .00000E+00 .39866E+03
.00000E+00 -.15946E+04 .00000E+00 .00000E+00 .15946E+04 .00000E+00
.39866E+03 .00000E+00 -.11074E+02 .39866E+03 .00000E+00 .11074E+02
    
```

MEMBER	NP1	NP2	NP3	NP4	NP5	NP6	H	V	A	I	L	COS	SIN
4	10	11	12	13	14	15	66.0000	.0000	63.7500	191.2500	66.0000	1.00000000	.00000000

THE STIFFNESS MATRIX FOR MEMBER 4

```

.20875E+05 .00000E+00 -.47444E+03 .10438E+05 .00000E+00 .47444E+03
.00000E+00 .17396E+04 .00000E+00 .00000E+00 -.17396E+04 .00000E+00
-.47444E+03 .00000E+00 .14377E+02 -.47444E+03 .00000E+00 -.14377E+02
.10438E+05 .00000E+00 -.47444E+03 .20875E+05 .00000E+00 .47444E+03
.00000E+00 -.17396E+04 .00000E+00 .00000E+00 .17396E+04 .00000E+00
.47444E+03 .00000E+00 -.14377E+02 .47444E+03 .00000E+00 .14377E+02
    
```

THE STRUCTURE STIFFNESS MATRIX BEFORE ADDING THE POST/DECK STIFFNESS MATRIX

```

.20875E+05 .00000E+00 -.47444E+03 .10438E+05 .00000E+00 .47444E+03 .00000E+00 .00000E+00 .00000E+00 .00000E+00
.00000E+00 .00000E+00 .00000E+00 .00000E+00 .00000E+00 .00000E+00 .00000E+00 .00000E+00 .00000E+00 .00000E+00
.00000E+00 .17396E+04 .00000E+00 .00000E+00 -.17396E+04 .00000E+00 .00000E+00 .00000E+00 .00000E+00 .00000E+00
.00000E+00 .00000E+00 .00000E+00 .00000E+00 .00000E+00 .00000E+00 .00000E+00 .00000E+00 .00000E+00 .00000E+00
-.47444E+03 .00000E+00 .14377E+02 -.47444E+03 .00000E+00 -.14377E+02 .00000E+00 .00000E+00 .00000E+00 .00000E+00
.00000E+00 .00000E+00 .00000E+00 .00000E+00 .00000E+00 .00000E+00 .00000E+00 .00000E+00 .00000E+00 .00000E+00
.10438E+05 .00000E+00 -.47444E+03 .40011E+05 .00000E+00 .75776E+02 .95678E+04 .00000E+00 .39866E+03 .00000E+00
.00000E+00 .00000E+00 .00000E+00 .00000E+00 .00000E+00 .00000E+00 .00000E+00 .00000E+00 .00000E+00 .00000E+00
.00000E+00 -.17396E+04 .00000E+00 .00000E+00 .33542E+04 .00000E+00 .00000E+00 -.15946E+04 .00000E+00 .00000E+00
.00000E+00 .00000E+00 .00000E+00 .00000E+00 .00000E+00 .00000E+00 .00000E+00 .00000E+00 .00000E+00 .00000E+00
.47444E+03 .00000E+00 -.14377E+02 .75776E+02 .00000E+00 .25451E+02 -.39866E+03 .00000E+00 -.11074E+02 .00000E+00
    
```

.00000E+00	.00000E+00	.00000E+00	.00000E+00	.00000E+00					
.00000E+00	.00000E+00	.00000E+00	.95678E+04	.00000E+00	-.39866E+03	.38271E+05	.00000E+00	.00000E+00	.95678E+04
.00000E+00	.39866E+03	.00000E+00	.00000E+00	.00000E+00					
.00000E+00	.00000E+00	.00000E+00	.00000E+00	-.15946E+04	.00000E+00	.00000E+00	.31893E+04	.00000E+00	.00000E+00
-.15946E+04	.00000E+00	.00000E+00	.00000E+00	.00000E+00					
.00000E+00	.00000E+00	.00000E+00	.39866E+03	.00000E+00	-.11074E+02	.00000E+00	.00000E+00	.22148E+02	-.39866E+03
.00000E+00	-.11074E+02	.00000E+00	.00000E+00	.00000E+00					
.00000E+00	.00000E+00	.00000E+00	.00000E+00	.00000E+00	.00000E+00	.95678E+04	.00000E+00	-.39866E+03	.40011E+05
.00000E+00	-.75778E+02	.10438E+05	.00000E+00	.47444E+03					
.00000E+00	.00000E+00	.00000E+00	.00000E+00	.00000E+00	.00000E+00	.00000E+00	-.15946E+04	.00000E+00	.00000E+00
.33342E+04	.00000E+00	.00000E+00	-.17396E+04	.00000E+00					
.00000E+00	.00000E+00	.00000E+00	.00000E+00	.00000E+00	.00000E+00	.39866E+03	.00000E+00	-.11074E+02	-.75778E+02
.00000E+00	.25451E+02	-.47444E+03	.00000E+00	-.14377E+02					
.00000E+00	.00000E+00	.00000E+00	.00000E+00	.00000E+00	.00000E+00	.00000E+00	.00000E+00	.00000E+00	.10438E+05
.00000E+00	-.47444E+03	.20875E+05	.00000E+00	.47444E+03					
.00000E+00	.00000E+00	.00000E+00	.00000E+00	.00000E+00	.00000E+00	.00000E+00	.00000E+00	.00000E+00	.00000E+00
-.17396E+04	.00000E+00	.00000E+00	.17396E+04	.00000E+00					
.00000E+00	.00000E+00	.00000E+00	.00000E+00	.00000E+00	.00000E+00	.00000E+00	.00000E+00	.00000E+00	.47444E+03
.00000E+00	-.14377E+02	.47444E+03	.00000E+00	.14377E+02					

THE POST/DECK STIFFNESS MATRIX

2.8334	-1.7213	.1162	.1782	-.0545
-1.7213	4.1621	-1.5211	-.2213	.1118
.1162	-1.5211	3.0455	-1.4359	.2425
.1782	-.2213	-1.4359	4.0794	-1.7776
-.0545	.1118	.2425	-1.7776	2.8483

THE STRUCTURE STIFFNESS MATRIX AFTER ADDING THE POST/DECK STIFFNESS MATRIX

.20875E+05	.00000E+00	-.47444E+02	.10438E+05	.00000E+00	.47444E+03	.00000E+00	.00000E+00	.00000E+00	.00000E+00
.00000E+00	.00000E+00	.00000E+00	.00000E+00	.00000E+00					
.00000E+00	.17396E+04	.00000E+00	.00000E+00	-.17396E+04	.00000E+00	.00000E+00	.00000E+00	.00000E+00	.00000E+00
.00000E+00	.00000E+00	.00000E+00	.00000E+00	.00000E+00					

-.47444E+03	.00000E+00	.17210E+02	-.47444E+03	.00000E+00	-.16098E+02	.00000E+00	.00000E+00	.11620E+00	.00000E+00
.00000E+00	.17820E+00	.00000E+00	.00000E+00	-.54500E-01					
.10438E+05	.00000E+00	-.47444E+03	.40011E+05	.00000E+00	.75778E+02	.95678E+04	.00000E+00	.39866E+03	.00000E+00
.00000E+00	.00000E+00	.00000E+00	.00000E+00	.00000E+00					
.00000E+00	-.17396E+04	.00000E+00	.00000E+00	.33342E+04	.00000E+00	.00000E+00	-.15946E+04	.00000E+00	.00000E+00
.00000E+00	.00000E+00	.00000E+00	.00000E+00	.00000E+00					
.47444E+03	.00000E+00	-.16098E+02	.75778E+02	.00000E+00	.29613E+02	-.39666E+03	.00000E+00	-.12595E+02	.00000E+00
.00000E+00	-.22130E+00	.00000E+00	.00000E+00	.11180E+00					
.00000E+00	.00000E+00	.00000E+00	.95678E+04	.00000E+00	-.39866E+03	.38271E+05	.00000E+00	.00000E+00	.95678E+04
.00000E+00	.39866E+03	.00000E+00	.00000E+00	.00000E+00					
.00000E+00	.00000E+00	.00000E+00	.00000E+00	-.15946E+04	.00000E+00	.00000E+00	.31893E+04	.00000E+00	.00000E+00
-.15946E+04	.00000E+00	.00000E+00	.00000E+00	.00000E+00					
.00000E+00	.00000E+00	.11620E+00	.39666E+03	.00000E+00	-.12595E+02	.00000E+00	.00000E+00	.25193E+02	-.39666E+03
.00000E+00	-.12510E+02	.00000E+00	.00000E+00	.24250E+00					
.00000E+00	.00000E+00	.00000E+00	.00000E+00	.00000E+00	.00000E+00	.95678E+04	.00000E+00	-.39866E+03	.40011E+05
.00000E+00	-.75778E+02	.10438E+05	.00000E+00	.47444E+03					
.00000E+00	-.15946E+04	.00000E+00	.00000E+00						
.33342E+04	.00000E+00	.00000E+00	-.17396E+04	.00000E+00					
.00000E+00	.00000E+00	.17820E+00	.00000E+00	.00000E+00	-.22130E+00	.39666E+03	.00000E+00	-.12510E+02	-.75778E+02
.00000E+00	.29613E+02	-.47444E+03	.00000E+00	-.16154E+02					
.00000E+00	.10438E+05								
.00000E+00	-.47444E+03	.20875E+05	.00000E+00	.47444E+03					
.00000E+00									
-.17396E+04	.00000E+00	.00000E+00	.17396E+04	.00000E+00					
.00000E+00	.00000E+00	-.54500E-01	.00000E+00	.00000E+00	.11180E+00	.00000E+00	.00000E+00	.24250E+00	.47444E+03
.00000E+00	-.16154E+02	.47444E+03	.00000E+00	.17225E+02					

THE MATRIX P

ROW 1	.00000000E+00	.00000000E+00	.00000000E+00
ROW 2	.00000000E+00	.00000000E+00	.00000000E+00
ROW 3	.00000000E+00	-.10000000E+01	.00000000E+00
ROW 4	.00000000E+00	.00000000E+00	.00000000E+00
ROW 5	.00000000E+00	.00000000E+00	.00000000E+00
ROW 6	.00000000E+00	.00000000E+00	-.20000000E+01
ROW 7	.00000000E+00	.00000000E+00	.00000000E+00
ROW 8	.00000000E+00	.00000000E+00	.00000000E+00
ROW 9	-.30000000E+01	.00000000E+00	.00000000E+00
ROW 10	.00000000E+00	.00000000E+00	.00000000E+00
ROW 11	.00000000E+00	.00000000E+00	.00000000E+00
ROW 12	.00000000E+00	.00000000E+00	.00000000E+00

ROW 13	.00000000E+00	.00000000E+00	.00000000E+00
ROW 14	.00000000E+00	.00000000E+00	.00000000E+00
ROW 15	.00000000E+00	.00000000E+00	.00000000E+00

THE MATRIX X

ROW 1	.64671963E-02	-.31965131E-02	.33264130E-02
ROW 2	.00000000E+00	.00000000E+00	.00000000E+00
ROW 3	-.42193991E+00	-.48420811E+00	-.57311867E+00
ROW 4	.65333672E-02	-.25910088E-02	.21455295E-03
ROW 5	.00000000E+00	.00000000E+00	.00000000E+00
ROW 6	-.85110962E+00	-.28655933E+00	-.72420100E+00
ROW 7	-.13640558E-03	-.15582421E-02	-.35674573E-02
ROW 8	.00000000E+00	.00000000E+00	.00000000E+00
ROW 9	-.11626464E+01	-.14064630E+00	-.56740642E+00
ROW 10	-.67596382E-02	-.90387078E-03	-.34404750E-02
ROW 11	.00000000E+00	.00000000E+00	.00000000E+00
ROW 12	-.83258418E+00	-.53090978E-01	-.30430297E+00
ROW 13	-.66708054E-02	-.64522885E-03	-.29690919E-02
ROW 14	.00000000E+00	.00000000E+00	.00000000E+00
ROW 15	-.39035671E+00	-.48157510E-02	-.97972476E-01

THE MATRIX OF LATERAL RAIL DISPLACEMENTS

-.4219E+00	-.4842E+00	-.5731E+00
-.8511E+00	-.2866E+00	-.7242E+00
-.1163E+01	-.1406E+00	-.5674E+00
-.8326E+00	-.5309E-01	-.3043E+00
-.3904E+00	-.4816E-02	-.9797E-01

THE MATRIX OF POST FORCES

.7302E-02	-.9042E+00	-.4921E+00
-.9070E+00	-.1341E+00	-.1108E+01
-.1194E+01	.2635E-01	-.2799E+00
-.9199E+00	-.2894E-01	-.1943E+00
.1405E-01	.4090E-01	.7455E-01